INTERNATIONAL TELECOMMUNICATION UNION

ITU-T

TELECOMMUNICATION
STANDARDIZATION SECTOR
OF ITU

G.8251
(11/2001)

SERIES G: TRANSMISSION SYSTEMS AND MEDIA, DIGITAL SYSTEMS AND NETWORKS

Digital networks – Quality and availability targets

The control of jitter and wander within the optical transport network (OTN)

ITU-T Recommendation G.8251

ITU-T G-SERIES RECOMMENDATIONS

TRANSMISSION SYSTEMS AND MEDIA, DIGITAL SYSTEMS AND NETWORKS

INTERNATIONAL TELEPHONE CONNECTIONS AND CIRCUITS	G.100–G.199
GENERAL CHARACTERISTICS COMMON TO ALL ANALOGUE CARRIER-TRANSMISSION SYSTEMS	G.200–G.299
INDIVIDUAL CHARACTERISTICS OF INTERNATIONAL CARRIER TELEPHONE SYSTEMS ON METALLIC LINES	G.300–G.399
GENERAL CHARACTERISTICS OF INTERNATIONAL CARRIER TELEPHONE SYSTEMS ON RADIO-RELAY OR SATELLITE LINKS AND INTERCONNECTION WITH METALLIC LINES	G.400–G.449
COORDINATION OF RADIOTELEPHONY AND LINE TELEPHONY	G.450–G.499
TESTING EQUIPMENTS	G.500–G.599
TRANSMISSION MEDIA CHARACTERISTICS	G.600–G.699
DIGITAL TERMINAL EQUIPMENTS	G.700–G.799
DIGITAL NETWORKS	G.800–G.899
DIGITAL SECTIONS AND DIGITAL LINE SYSTEM	G.900–G.999
QUALITY OF SERVICE AND PERFORMANCE	G.1000–G.1999
TRANSMISSION MEDIA CHARACTERISTICS	G.6000–G.6999
DIGITAL TERMINAL EQUIPMENTS	G.7000–G.7999
DIGITAL NETWORKS	G.8000–G.8999
General aspects	G.8000–G.8099
Design objectives for digital networks	G.8100–G.8199
Quality and availability targets	**G.8200–G.8299**
Network capabilities and functions	G.8300–G.8399
SDH network characteristics	G.8400–G.8499
Management of transport network	G.8500–G.8599
SDH radio and satellite systems integration	G.8600–G.8699
Optical transport networks	G.8700–G.8799

For further details, please refer to the list of ITU-T Recommendations.

ITU-T Recommendation G.8251

The control of jitter and wander within the optical transport network (OTN)

Summary

This Recommendation specifies the maximum network limits of jitter and wander that shall not be exceeded and the minimum equipment tolerance to jitter and wander that shall be provided at any relevant interfaces which are based on the Optical Transport Network (OTN).

The requirements for the jitter and wander characteristics that are specified in this Recommendation must be adhered to in order to ensure interoperability of equipment produced by different manufacturers and a satisfactory network performance.

Source

ITU-T Recommendation G.8251 was prepared by ITU-T Study Group 15 (2001-2004) and approved under the WTSA Resolution 1 procedure on 29 November 2001.

Keywords

Frequency accuracy, input jitter tolerance, input wander tolerance, jitter generation, jitter transfer, network limits, ODUk clock, output jitter, output wander, pull-in range, pull-out range, wander generation.

FOREWORD

The International Telecommunication Union (ITU) is the United Nations specialized agency in the field of telecommunications. The ITU Telecommunication Standardization Sector (ITU-T) is a permanent organ of ITU. ITU-T is responsible for studying technical, operating and tariff questions and issuing Recommendations on them with a view to standardizing telecommunications on a worldwide basis.

The World Telecommunication Standardization Assembly (WTSA), which meets every four years, establishes the topics for study by the ITU-T study groups which, in turn, produce Recommendations on these topics.

The approval of ITU-T Recommendations is covered by the procedure laid down in WTSA Resolution 1.

In some areas of information technology which fall within ITU-T's purview, the necessary standards are prepared on a collaborative basis with ISO and IEC.

NOTE

In this Recommendation, the expression "Administration" is used for conciseness to indicate both a telecommunication administration and a recognized operating agency.

INTELLECTUAL PROPERTY RIGHTS

ITU draws attention to the possibility that the practice or implementation of this Recommendation may involve the use of a claimed Intellectual Property Right. ITU takes no position concerning the evidence, validity or applicability of claimed Intellectual Property Rights, whether asserted by ITU members or others outside of the Recommendation development process.

As of the date of approval of this Recommendation, ITU had not received notice of intellectual property, protected by patents, which may be required to implement this Recommendation. However, implementors are cautioned that this may not represent the latest information and are therefore strongly urged to consult the TSB patent database.

CONTENTS

Page

Introduction

In an OTN, jitter and wander accumulate on transmission paths according to the jitter and wander generation and transfer characteristics of each respective equipment interconnected. This equipment may be, for example, 3R regenerators, client mappers, and client demappers/desynchronizers.

An excessive amount of jitter and wander can adversely affect both digital (e.g. by generation of bit errors, frame slips and other abnormalities) and analogue baseband signals (e.g. by unwanted phase modulation of the transmitted signal). The consequences of such impairment will, in general, depend on the particular service that is being carried and the terminating or adaptation equipment involved.

It is therefore necessary to set limits on the maximum magnitude of jitter and wander, and the corresponding minimum jitter and wander tolerance at network interfaces, in order to guarantee a proper quality of the transmitted signals and a proper design of the equipment.

These network limits are independent of the particular service that is being carried.

ITU-T Recommendation G.8251

The control of jitter and wander within the optical transport network (OTN)

1 Scope

The scope of this Recommendation is to define the parameters and the relevant limits that satisfactorily control the amount of jitter and wander present at the OTN network-node interface (NNI).

OTN network interfaces, to which this Recommendation is applicable, are defined in terms of bit rates and frame structures in ITU-T Rec. G.709; the relevant equipment characteristics are described in ITU-T Rec. G.798 and the optical characteristics in ITU-T Rec. G.959.1. Additional information regarding the architecture of the OTN is found in ITU-T Rec. G.872.

Network limits given in clause 5, OTN interface tolerance specifications in 6.1, and OTN equipment interface specifications in Annex A apply at or refer to the OTUk interface. The relevant bit rates for these specifications are the OTUk bit rates. Note that some of the other requirements in this Recommendation, e.g. the demapper clock (ODCp), asynchronous mapper clock (ODCa), and bit-synchronous mapper clock (ODCb) requirements in Annex A, apply to other interfaces and other bit rates (i.e. the demapper resides in the sink adaptation function between the ODUkP and CBR client, while the asynchronous and bit-synchronous mapper clocks reside in the source adaptation function between the ODUkP and client). In this Recommendation the term *clock*, when used in ODU clock (ODC), refers to a frequency source.

The OTN physical layer is not required to transport network synchronization. More precisely, neither the ODUk nor any layers below it are required to transport synchronization. *Network synchronization distribution is a function of the client layer, e.g. SDH.* ITU-T Rec. G.825 provides the jitter and wander requirements for SDH clients, and any SDH signal (which must meet G.825) is suitable for providing synchronization (see ITU-T Rec. G.803). SDH clients must meet ITU-T Rec. G.825 requirements for both asynchronous and bit-synchronous mappings.

Jitter and wander requirements for SDH networks are specified in ITU-T Rec. G.825. Jitter and wander requirements for PDH and synchronization networks are specified in ITU-T Rec. G.823, for networks based on the first level bit rate of 2048 kbit/s, and in ITU-T Rec. G.824 for networks based on the first-level bit rate of 1544 kbit/s.

The jitter and wander control philosophy is based on the need:

– to recommend a maximum network limit that should not be exceeded at any relevant OTN NNI;
– to recommend a consistent framework for the specification of individual digital equipment (i.e. jitter and wander transfer, tolerance and generation requirements);
– to provide sufficient information and guidelines for organizations to measure and study jitter and wander accumulation in any network configuration.

Note that there may exist hybrid NE types that contain both SDH and OTN atomic functions. For such hybrid NEs it may not be possible to access the respective ports to make measurements to verify compliance with the requirements in this Recommendation. Measurements to verify compliance for hybrid NE types is outside the scope of this Recommendation.

2 References

The following ITU-T Recommendations and other references contain provisions which, through reference in this text, constitute provisions of this Recommendation. At the time of publication, the editions indicated were valid. All Recommendations and other references are subject to revision; users of this Recommendation are therefore encouraged to investigate the possibility of applying the most recent edition of the Recommendations and other references listed below. A list of the currently valid ITU-T Recommendations is regularly published.

[1] ITU-T Recommendation G.709/Y.1331 (2001), *Interfaces for the optical transport network (OTN)*.

[2] ITU-T Recommendation G.798 (2002), *Characteristics of optical transport network hierarchy equipment functional blocks*.

[3] ITU-T Recommendation G.959.1 (2001), *Optical Transport Network Physical Layer Interfaces*.

[4] ITU-T Recommendation G.825 (2000), *The control of jitter and wander within digital networks which are based on the synchronous digital hierarchy (SDH)*.

[5] ITU-T Recommendation G.783 (2000), *Characteristics of synchronous digital hierarchy (SDH) equipment functional blocks*.

[6] ITU-T Recommendation G.810 (1996), *Definitions and terminology for synchronization networks*.

[7] ITU-T Recommendation G.823 (2000), *The control of jitter and wander within digital networks which are based on the 2048 kbit/s hierarchy*.

[8] ITU-T Recommendation G.824 (2000), *The control of jitter and wander within digital networks which are based on the 1544 kbit/s hierarchy*.

[9] ITU-T Recommendation G.707/Y.1322 (2000), *Network node interface for the synchronous digital hierarchy (SDH)*.

[10] ITU-T Recommendation G.872 (2002), *Architecture of optical transport networks*.

[11] ITU-T Recommendation O.171 (1997), *Timing jitter and wander measuring equipment for digital systems which are based on the plesiochronous digital hierarchy (PDH)*.

[12] ITU-T Recommendation O.172 (2001), *Jitter and wander measuring equipment for digital systems which are based on the synchronous digital hierarchy (SDH)*.

[13] ITU-T Recommendation G.803 (2000), *Architecture of transport networks based on the synchronous digital hierarchy (SDH)*.

[14] ITU-T Recommendation G.811 (1997), *Timing characteristics of primary reference clocks*.

3 Definitions

The terms and definitions used in this Recommendation that pertain to timing and jitter are contained in ITU-T Recs G.810 and G.825. The terms and definitions used in this Recommendation that pertain to the OTN are contained in ITU-T Recs G.709, G.798, and G.872. The terms and definitions used in the Recommendation that pertain to SDH are contained in ITU-T Recs G.707, G.783, and G.803.

4 Abbreviations and Acronyms

This Recommendation uses the following abbreviations:

3R	Reamplification, Reshaping and Retiming
A	Adaptation
AI	Adapted Information
AIS	Alarm Indication Signal
AP	Access Point
CBR	Constant Bit Rate
CI	Characteristic Information
CK	Clock
CP	Connection Point
D	Data
FEC	Forward Error Correction
MC	Master Clock
MTIE	Maximum Time Interval Error
NE	Network Element
NNI	Network Node Interface
OA	Optical Amplifier
OCh	Optical Channel with full functionality
OChr	Optical Channel with reduced functionality
ODC	ODUk Clock
ODCx	ODUk Clock of type "x", where x is "a", "b", "r", or "p"
ODU	Optical Channel Data Unit
ODUk	Optical Channel Data Unit-k
ODUkP	ODUk Path
ODUkT	ODUk Tandem connection
OMS	Optical Multiplex Section
OPU	Optical Channel Payload Unit
OPUk	Optical Channel Payload Unit-k
OTM	Optical Transport Module
OTN	Optical Transport Network
OTS	Optical Transmission Section
OTU	Optical channel Transport Unit
OTUk	completely standardized Optical channel Transport Unit-k
PDH	Plesiochronous Digital Hierarchy
PI	Proportional plus Integral
PLL	Phase-Locked Loop

PMD	Polarization Mode Dispersion
ppm	parts per million
PRBS	Pseudo-Random Binary Sequence
PRC	Primary Reference Clock
PSD	Power Spectral Density
rms	root mean square
RS	Reed-Solomon
SDH	Synchronous Digital Hierarchy
SEC	SDH Equipment Clock
Sk	Sink
So	Source
SSU	Synchronization Supply Unit
STM	Synchronous Transport Module
STM-N	Synchronous Transport Module – level N
TCP	Termination Connection Point
TDEV	Time Deviation
UI	Unit Interval
UIpp	Unit Interval peak-to-peak
UTC	Coordinated Universal Time
VCO	Voltage-Controlled Oscillator
WFM	White Frequency Modulation
WPM	White Phase Modulation

5 Network limits for the maximum output jitter and wander at an OTUk interface

The jitter and wander limits given in this clause are the maximum permissible levels at OTUk interfaces within an OTN. The OTUk interface is just below the OCh/OTUk adaptation function in Figure 1-3/G.798 [2]. One example of this interface is the input to a 3R regenerator (sink) or output from a 3R regenerator (source).

NOTE – The OTUk is precisely defined in ITU-T Rec. G.709; essentially, it is the digital signal that is mapped into the Optical Channel (OCh). The OTUk bit rate is essentially the line rate associated with the OCh and respective wavelength that the OCh is assigned to. The OTUk bit rates are given in Table 7-1/G.709, and are equal to the inverses of the bit periods given in Table 1.

Table 1/G.8251 – Maximum permissible jitter at OTUk interfaces

Interface	Measurement bandwidth, –3 dB frequencies (Hz)	Peak-to-peak amplitude (UIpp)
OTU1	5 k to 20 M	1.5
	1 M to 20 M	0.15
OTU2	20 k to 80 M	1.5
	4 M to 80 M	0.15
OTU3	20 k to 320 M	6.0
	16 M to 320 M	0.15

NOTE – OTU1 $1\text{ UI} = \dfrac{238}{(255)(2.48832)}\text{ ns} = 375.1\text{ ps}$

OTU2 $1\text{ UI} = \dfrac{237}{(255)(9.95328)}\text{ ns} = 93.38\text{ ps}$

OTU3 $1\text{ UI} = \dfrac{236}{(255)(39.81312)}\text{ ns} = 23.25\text{ ps}$

5.1 Network limits for jitter

Table 1 gives the maximum permissible levels of jitter at OTUk interfaces. Jitter as measured over a 60-second interval shall not exceed the limits given in Table 1, when using the specified measurement filters. The limits shall be met for all operating conditions and regardless of the amount of equipment preceding the interface. In general, these network limits are compatible with the minimum tolerance to jitter that all equipment input ports are required to provide. Guidelines for the derivation of the parameters values of Table 1 are given in Appendix I.

There is a close relationship between network limits and input tolerance such that the jitter measurement filter cut-off frequencies used in Table 1 have the same values as the jitter tolerance mask corner frequencies used in 6.1. Appendix I provides further information about this relationship.

The high-pass measurement filters of Table 1 have a first-order characteristic and a roll-off of 20 dB/decade. The low-pass measurement filters have a maximally-flat, Butterworth characteristic and a roll-off of −60 dB/decade.

5.2 Network limits for wander

OTUk interfaces are not synchronization interfaces. None of the ODUk clocks are significant sources of wander. There is no need for specification of network wander limits.

6 Jitter and wander tolerance of network interfaces

6.1 Jitter and wander tolerance of OTN interfaces

This clause specifies the jitter and wander tolerance for OTUk input ports. This is the minimum jitter and wander that must be tolerated at the input to the OCh/OTUk_A_Sk atomic function. This represents, for example, the jitter and wander tolerance for a 3R regenerator. The input ports of all equipment must be capable of accommodating levels of jitter and wander up to at least the minimum limits defined in 6.1.1, 6.1.2, and 6.1.3 in order to ensure that, in general, any equipment can be connected to any appropriate interface within a network.

NOTE 1 – As stated above, both the jitter and wander tolerance requirements apply at the OTUk input port, which is the input to the OCh/OTUk_A_Sk atomic function. However, while the requirements apply at this interface, they are not all driven by this atomic function. For example, the highband jitter tolerance requirement (i.e. the tolerance above the highest frequency breakpoint, which is 1 MHz for OTU1, 4 MHz for OTU2, and 16 MHz for OTU3) is driven by the wideband clock recovery circuit in the OCh/OTUk_A_Sk atomic function; however, the wideband jitter tolerance requirement (i.e. the tolerance between 5 kHz and 100 kHz for OTU1 and between 20 kHz and 400 kHz for OTU2 and OTU3) is driven by the ODCr in the OTUk/ODUk_A_So and OTUk/ODUk_A_Sk atomic functions.

The jitter and wander tolerance of an OTUk interface indicates the minimum level of phase noise that the input port shall accommodate whilst:

- not causing any alarms;
- not causing any slips or loss of lock in the clock recovery phase-locked loop; and
- not causing any bit errors in excess of those allowed by an equivalent 1 dB optical power penalty.

The limit of tolerable input jitter is measured by the 1 dB Optical Power Penalty Method as follows:

The optical input power is reduced until a BER of 10^{-10} is reached. Then the power is increased by 1 dB and jitter is applied to the input signal. The amount of jitter that results in BER of 10^{-10} is the limit of tolerable input jitter. If the system uses FEC this shall be disabled for the measurement when using an external bit error detector. Alternatively, BER may be measured by leaving the FEC enabled and counting the number of corrected bit errors per unit time.

NOTE 2 – This definition is subject to further study, taking into account the effects of, e.g. Optical Amplifiers (OA), Polarisation Mode Dispersion (PMD), and Forward Error Correction (FEC).

All OTUk input ports of equipment shall be able to tolerate an OCh_AI_D signal that has:

a) optical characteristics of ITU-T Rec. G.959.1;

b) a frequency offset (relative to the nominal value) within the range defined in A.3.

c) a sinusoidal phase deviation having an amplitude-frequency relationship, defined in the following clauses, which indicates the appropriate limits for the different interfaces.

In principle, these requirements shall be met regardless of the information content of the digital signal. However, for test purposes, the content of the signal with jitter and wander modulation should be a structured test sequence as defined in ITU-T Rec. G.709.

For convenience of testing, the required tolerance is defined in terms of the peak-to-peak amplitude and frequency of sinusoidal jitter which modulates a digital test pattern. It is important to recognize that this test condition is not, in itself, intended to be representative of the type of jitter found in practice in a network.

Guidance on the measurement set-up for input jitter and wander tolerance is provided in Appendix III/G.823.

Requirements for jitter and wander tolerance for each OTUk rate are given in the following subclauses. These requirements specify the minimum levels of jitter that must be accommodated at an OTUk interface.

6.1.1 OTU1 jitter and wander tolerance

The level of sinusoidal jitter that must be accommodated by OTU1 interfaces is specified in Table 2 and illustrated in Figure 1. A phase-locked loop with corner frequency greater than or equal to 5 kHz that can tolerate jitter and wander indicated by the 20 dB/decade sloped portion of the mask between 500 Hz and 5 kHz will also tolerate jitter and wander indicated by an extension of this sloped region to lower frequencies, because such jitter and wander is within the bandwidth of the phase-locked loop. OTU1 interfaces must tolerate this jitter and wander but, for practical reasons, it is not required to measure them below 500 Hz.

Table 2/G.8251 – OTU1 input sinusoidal jitter tolerance limit

Frequency f (Hz)	Peak-to-peak amplitude (UIpp)
$500 < f \leq 5$ k	$7500 f^{-1}$
5 k $< f \leq 100$ k	1.5
100 k $< f \leq 1$ M	$1.5 \times 10^5 f^{-1}$
1 M $< f \leq 20$ M	0.15

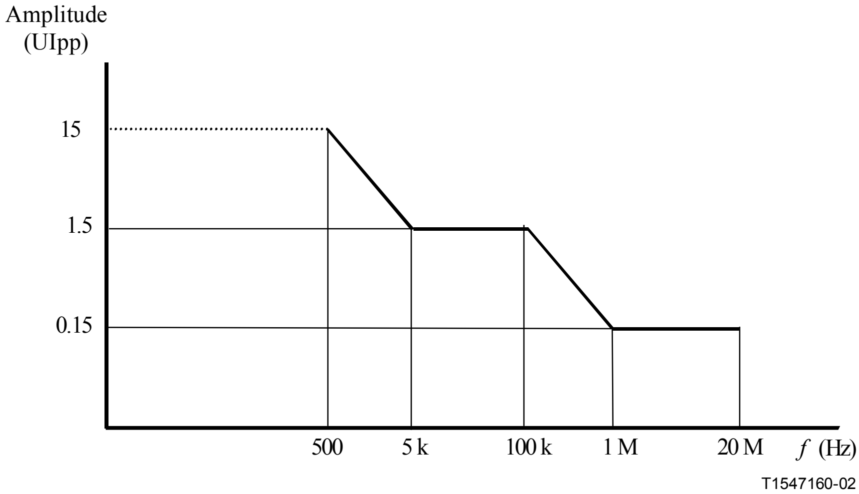

Figure 1/G.8251 – OTU1 input sinusoidal jitter tolerance limit

6.1.2 OTU2 jitter and wander tolerance

The level of sinusoidal jitter that must be accommodated by OTU2 interfaces is specified in Table 3 and illustrated in Figure 2. A phase-locked loop with corner frequency greater than or equal to 20 kHz that can tolerate jitter and wander indicated by the 20 dB/decade sloped portion of the mask between 2 kHz and 20 kHz will also tolerate jitter and wander indicated by an extension of this sloped region to lower frequencies, because such jitter and wander is within the bandwidth of the phase-locked loop. OTU2 interfaces must tolerate this jitter and wander but, for practical reasons, it is not required to measure them below 2 kHz.

Table 3/G.8251 – OTU2 Input sinusoidal jitter tolerance limit

Frequency f (Hz)	Peak-to-peak amplitude (UIpp)
2 k $< f \leq 20$ k	$3.0 \times 10^4 f^{-1}$
20 k $< f \leq 400$ k	1.5
400 k $< f \leq 4$ M	$6.0 \times 10^5 f^{-1}$
4 M $< f \leq 80$ M	0.15

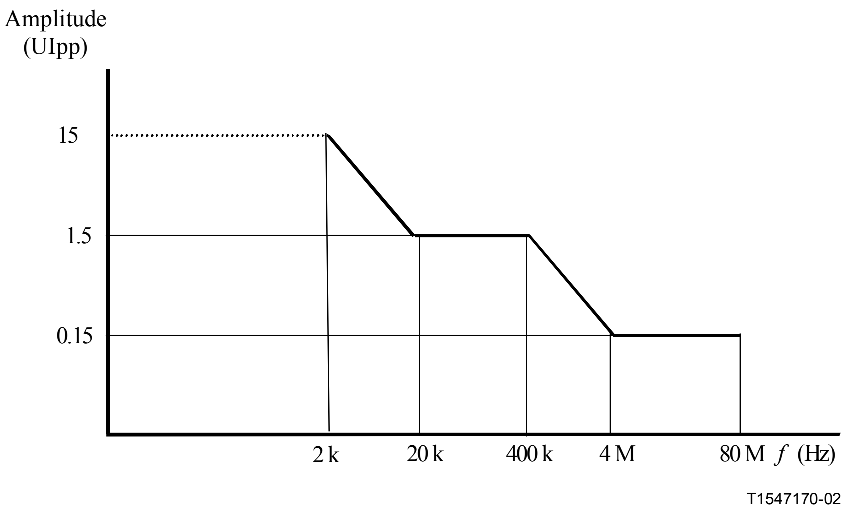

Figure 2/G.8251 – OTU2 Input sinusoidal jitter tolerance limit

6.1.3 OTU3 jitter and wander tolerance

The level of sinusoidal jitter that must be accommodated by OTU3 interfaces is specified in Table 4 and illustrated in Figure 3. A phase-locked loop with corner frequency greater than or equal to 20 kHz that can tolerate jitter and wander indicated by the 20 dB/decade sloped portion of the mask between 8kHz and 20 kHz will also tolerate jitter and wander indicated by an extension of this sloped region to lower frequencies, because such jitter and wander is within the bandwidth of the phase-locked loop. OTU3 interfaces must tolerate this jitter and wander but, for practical reasons, it is not required to measure it below 8 kHz.

Table 4/G.8251 – OTU3 input sinusoidal jitter tolerance limit

Frequency f (Hz)	Peak-to-peak amplitude (UIpp)
8 k < f ≤ 20 k	$1.2 \times 10^5 f^{-1}$
20 k < f ≤ 400 k	6.0
400 k < f ≤ 16 M	$2.4 \times 10^6 f^{-1}$
16 M < f ≤ 320 M	0.15

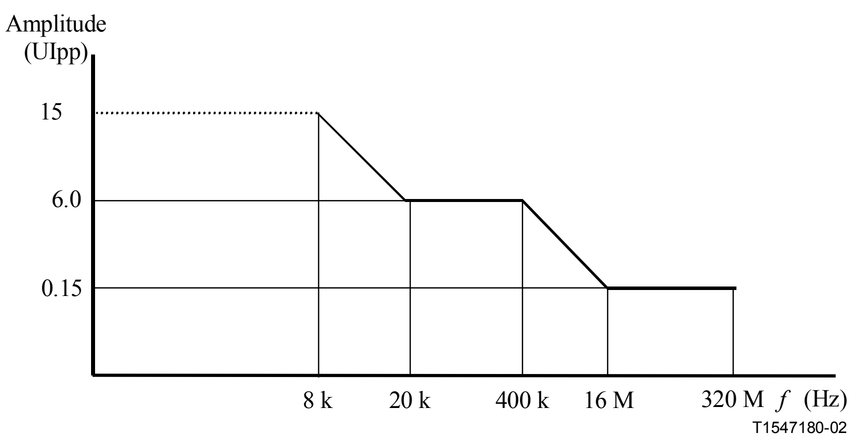

Figure 3/G.8251 – OTU3 input sinusoidal jitter tolerance limit

6.2 Jitter and wander tolerance of CBR2G5, CBR10G, and CBR40G client interfaces

Jitter and wander tolerance requirements and network limits for CBR2G5, CBR10G, and CBR40G are derived from the corresponding requirements for STM-16 and STM-64 signals, respectively, given in ITU-T Rec. G.825.

NOTE – Jitter and wander tolerance requirements and network limits for STM-256 signals are not currently given in ITU-T Rec. G.825; however, it is expected they will be in future editions of ITU-T Rec. G.825.

STM input ports, i.e. the input to the ODUkP/CBRx-a_A_So and ODUkP/CBRx-b_A_So atomic functions, for the case where the STM client is STM-16, STM-64, or STM-256, must tolerate jitter and wander levels specified in ITU-T Rec. G.825. Guidelines for measuring the input jitter and wander tolerance of equipment input interfaces are given in Appendix III/G.823.

Annex A

Specification of the ODUk clock (ODC)

A.1 Scope

This annex contains the requirements for the ODUk Clock (ODC). Here, the term *clock* refers to a clock filtering and/or generating circuit. Four ODC types are defined, for different applications (see A.2):

1) ODCa for asynchronous mapping of clients into ODUk;

2) ODCb for bit-synchronous mapping of clients into ODUk;

3) ODCr for 3R regeneration; and

4) ODCp for demapping of constant bit rate (CBR) clients.

The ODCa and ODCb generate the timing signal for the ODUk and OTUk signals produced by an OTN network element. The ODCr generates the timing signal for the OTUk produced by a 3R regenerator. The ODCp generates the timing signal for a demapped CBR client signal.

The four ODC types, the atomic functions they reside in, and their applicable requirements, are summarized in Table A.1. The requirements are described in more detail in the clauses that follow.

Table A.1/G.8251 – Summary of ODUk Clock (ODC) types

	ODCa	ODCb	ODCr	ODCp
Atomic function	ODUkP/CBRx-a_A_So ODUkP/ATM_A_So ODUkP/GFP_A_So ODUkP/NULL_A_So ODUkP/PRBS_A_So ODUkP/non-specific-client-bitstream_A_So	ODUkP/CBRx-b_A_So	OTUk/ODUk_A_So and OTUk/ODUk_A_Sk (i.e. the clocks of these atomic functions are concentrated in a single ODCr; see ITU-T Rec. G.798)	ODUkP/CBRx_A_Sk
Frequency accuracy	±20 ppm	±20 ppm	±20 ppm	±20 ppm
Free-run mode supported	yes	yes	yes	yes
Locked mode supported	no	yes	yes	yes
Holdover mode supported	no	no	no	no
Pull-in range	NA	±20 ppm	±20 ppm	±20 ppm
Pull-out range	NA	±20 ppm	±20 ppm	±20 ppm
Jitter generation	Table A.2	Table A.2	Table A.2	Table A.3
Wander generation	NA	NA (Note 1)	NA	NA (Note 2)
Jitter tolerance	NA	ITU-T Rec. G.825	Table 2, Figure 1 (OTU1); Table 3, Figure 2 (OTU2); Table 4, Figure 3 (OTU3)	Table 2, Figure 1 (OTU1); Table 3, Figure 2 (OTU2); Table 4, Figure 3 (OTU3)
Wander tolerance	NA	ITU-T Rec. G.825	Clause 6.1	Clause 6.1

Table A.1/G.8251 – Summary of ODUk Clock (ODC) types

	ODCa	ODCb	ODCr	ODCp
Jitter transfer	NA	Maximum bandwidth: ODU1: 1 kHz ODU2: 4 kHz ODU3: 16 kHz Maximum gain peaking: 0.1 dB for ODU1, 2, and 3 (see Table A.4 and Figure A.1)	Maximum bandwidth: OTU1: 250 kHz OTU2: 1000 kHz OTU3: 4000 kHz Maximum gain peaking: 0.1 dB for OTU1, 2, and 3 (see Table A.5 and Figure A.1)	Maximum bandwidth: 300 Hz for ODU1, 2, and 3 Maximum gain peaking: 0.1 dB for ODU1, 2, and 3 (see A.6.3)
Output when input signal is lost	AIS (SDH client) OTUk: no frame hit OTUk frequency unchanged	AIS (SDH client) OTUk: no frame hit OTUk initial frequency change ≤9 ppm	AIS (OTUk) OTUk: frame hit allowed Temporary OTUk frequency offset >20 ppm allowed	AIS (SDH client) Frequency offset ≤20 ppm
NA No requirement because not applicable NOTE 1 – The wander generation of ODCb is expected to be negligible compared to the wander on the input CBR (e.g. SDH) client signal, because the ODCb bandwidth is relatively wide band. NOTE 2 – The intrinsic wander generation of the ODCp is negligible compared to the wander generated by the demapping process.				

The output timing signals at the lower layers are derived from the ODUkP_AI_CK (i.e. from the ODCa, ODCb, or ODCr output) by frequency multiplication. For example, the OTUk timing signal is the OTUk_AI_CK, which is output from the OTUk/ODUk_A_So atomic function (see 13.3.1.1/G.798). This signal is derived from the ODUk_CI_CK (characteristic information of the ODUk; this signal has the same frequency as the ODUkP_AI_CK) via frequency multiplication by 255/239. The OTUk_AI_CK provides the timing input to the OCh/OTUk_A_So atomic function, whose output is the OCh data signal (OCh_AI_D).

NOTE – In the case of asynchronous mapping, there is no requirement for a single master clock, i.e. single ODCa, in OTN equipment. Within OTN equipment there may be multiple, independent ODCa clocks for each outgoing wavelength (i.e. for the source of each OCh, OTUk, and ODUk). In the case of bit-synchronous mapping, 3R regeneration, and demapping there cannot be a single master clock for multiple OChs, i.e. an ODCb, ODCr, or ODCp supplies timing for a single ODUk, OTUk, or CBR client, respectively.

A.2 Applications

The ODCa and ODCb are used for the mapping of payload to the ODUk signal; the ODCr is used for the 3R regeneration; the ODCp is used in the CBR demapper.

The ODCa, used for asynchronous mapping, is free-running and the bit rate offset is accommodated by appropriately controlled stuffing.

The ODCb, used for bit-synchronous mapping, is locked to the bit rate of the incoming payload signal and the bit rate offset is accommodated by a fixed stuff pattern. The synchronous operation is continued even if the received payload contents is AIS. If the incoming signal fails, the ODC enters the free-run condition.

The ODCr, used for 3R regeneration, is locked to the bit rate of the incoming OCh_AP signal (including AIS). If the incoming signal fails, the ODC enters the free-run condition.

The ODCp, used for the CBR demapper, is locked to the bit rate of the gapped OPUk clock (i.e. the timing of the signal that results from taking the OPUk payload and applying the justification control). If the incoming signal fails, the ODCp enters a free-run condition.

A.3 Frequency accuracy

Under free-running conditions, the output frequency accuracy of ODCa, ODCb, ODCr, and ODCp shall not be worse than 20 ppm with respect to a reference traceable to a G.811 clock.

A.4 Pull-in and pull-out ranges

A.4.1 Pull-in range

The minimum pull-in range of ODCb, ODCr, and ODCp shall be ±20 ppm, whatever the internal oscillator frequency offset may be. There is no requirement for the pull-in range of ODCa because it is free-running.

A.4.2 Pull-out range

The minimum pull-out range of ODCb, ODCr, and ODCp shall be ±20 ppm, whatever the internal oscillator frequency offset may be. There is no requirement for the pull-out range of ODCa because it is free-running.

A.5 Noise generation

This clause limits the output jitter and wander for each applicable clock type, in the absence of any input jitter or wander. Note that the respective input and output signals depend on the clock type, because the different clock types are located in different atomic functions.

A.5.1 Jitter generation

A.5.1.1 ODCa, ODCb, and ODCr jitter generation

In the absence of input jitter, jitter of the ODCa and ODCb output, i.e. the ODUkP_AI_CK signal, shall not exceed the values specified in Table A.2 when measured over a 60-second interval with the measurement filters specified in that table. Since ODCa is free-running, there is no input jitter by definition. For ODCb, it is the input client signal that is jitter-free.

Table A.2/G.8251 – ODCa, ODCb, and ODCr jitter generation requirements

Interface	Measurement bandwidth, –3 dB frequencies (Hz)	Peak-to-peak amplitude (UIpp) (Note 2)
ODU1, OTU1	5 k to 20 M	0.3
	1 M to 20 M	0.1
ODU2, OTU2	20 k to 80 M	0.3
	4 M to 80 M	0.1
ODU3, OTU3	20 k to 320 M	1.2 (Note 1)
	16 M to 320 M	0.1

NOTE 1 – See IV.4 for additional information.

NOTE 2 – OTU1 $1\ \mathrm{UI} = \dfrac{238}{(255)(2.48832)}\ \mathrm{ns} = 375.1\ \mathrm{ps}$

OTU2 $1\ \mathrm{UI} = \dfrac{237}{(255)(9.95328)}\ \mathrm{ns} = 93.38\ \mathrm{ps}$

OTU3 $1\ \mathrm{UI} = \dfrac{236}{(255)(39.81312)}\ \mathrm{ns} = 23.25\ \mathrm{ps}$

In the absence of input jitter to a 3R regenerator (i.e. to the OCh/OTUk_A_Sk atomic function), the output jitter on the clock information in the OCh_AI_D signal output from the OCh/OTUk_A_So atomic function shall not exceed the values specified in Table A.2 when measured over a 60-second interval with the measurement filters specified in that table. The signal that must be free of input jitter when this measurement is made is the OCh_AI_D signal input to the corresponding OCh/OTUk_A_Sk atomic function. Specifically, it is the clock information in this signal that must have no input jitter.

NOTE – This is actually a requirement for the jitter generation of a 3R regenerator; it constrains the total jitter generation in all the atomic functions from OCh/OTUk_A_Sk to OCh/OTUk_A_So (inclusive). The ODCr is included in this, as it resides in the OTUk/ODUk_A_So and OTUk/ODUk_A_Sk atomic functions (i.e. the clocks of these atomic functions are concentrated in a single ODCr; see ITU-T Rec. G.798).

A.5.1.2 ODCp jitter generation

In the absence of input jitter, jitter of the ODCp output, i.e. the STM_CI_CK signal, shall not exceed the values specified in Table A.3 when measured over a 60-second interval with the measurement filters specified in that table. Note that the output is at the CBRx_CP interface. The requirements shall be met when the input frequency of the STM-N client is constant within the limits −20 ppm to +20 ppm from the nominal frequency.

One purpose of the ODCp wideband jitter generation requirements is to ensure that the gaps due to fixed overhead in the OTUk frame will not cause excessive output jitter. Additional information on this is provided in V.3.

Table A.3/G.8251 – ODCp jitter generation requirements

Interface	Measurement bandwidth, –3 dB frequencies (Hz)	Peak-to-peak amplitude (UIpp) (Note 2)
STM-16	5 k to 20 M	1.0
	1 M to 20 M	0.1
STM-64	20 k to 80 M	1.0
	4 M to 80 M	0.1
STM-256	80 k to 320 M (Note 1)	1.0
	16 M to 320 M	0.1

NOTE 1 – Values for STM-256 are provisional and are not present in ITU-T Rec. G.825 at the time of publication of this Recommendation.

NOTE 2 – OTU1 $1\ \text{UI} = \dfrac{238}{(255)(2.48832)}\ \text{ns} = 375.1\ \text{ps}$

OTU2 $1\ \text{UI} = \dfrac{237}{(255)(9.95328)}\ \text{ns} = 93.38\ \text{ps}$

OTU3 $1\ \text{UI} = \dfrac{236}{(255)(39.81312)}\ \text{ns} = 23.25\ \text{ps}$

A.5.2 Wander generation

There are no wander generation requirements for ODCa, ODCb, ODCr, and ODCp. For ODCb, any intrinsic wander generation is expected to be negligible compared to the wander on the input CBR (e.g. SDH) client signal, because the ODCb bandwidth is relatively wide band. The intrinsic wander generation of the ODCp is negligible compared to the wander generated by the demapping process.

A.6 Noise tolerance

This clause specifies the jitter and wander tolerance of ODCb, ODCr, and ODCp. There are no jitter and wander tolerance requirements for ODCa because ODCa is free-running.

ODCb must satisfy the same jitter and wander tolerance requirements as STM-16, -64, and -256 client interfaces (the input to the ODUkP/CBRx-b_A_So atomic function). These requirements are given in 6.2, which references ITU-T Rec. G.825. Note that the ODCb is contained in the ODUkP/CBRx-b_A_So atomic function.

ODCr and ODCp must satisfy the same jitter and wander tolerance requirements as OTUk input ports (the input to the OCh/OTUk_A_Sk atomic function). These requirements are given in 6.1 and its subclauses. Note that the ODCr is contained in the OTUk/ODUk_A_So and OTUk/ODUk_A_Sk atomic functions, and the ODCp is contained in the ODUkP/CBRx_A_Sk atomic function.

A.7 Jitter transfer

This clause specifies the jitter transfer of ODCb, ODCr, and ODCp. There are no jitter transfer requirements for ODCa because ODCa is free-running.

A.7.1 Jitter transfer for ODCb

The jitter transfer function for ODCb is defined as the ratio of the output sinusoidal jitter amplitude to input sinusoidal jitter amplitude, as a function of frequency. The ODCb input is the CBRx_CI_CK signal at the ODUkP/CBRx-b_A_So atomic function. The ODCb output is the CBRx_AI_CK signal at the ODUkP/CBRx-b_A_So atomic function.

The jitter transfer function of ODCb shall be under the curve given in Figure A.1 when input sinusoidal jitter up to the respective masks referenced in A.6 is applied. The parameters of Figure A.1 are given in Table A.4. Note that the parameter f_C may be considered the maximum bandwidth of the ODCb, and the parameter P the maximum gain peaking of the ODCb. The jitter transfer limit is specified between frequencies of f_L and f_H. The jitter transfer limit is not specified for frequencies higher than f_H nor lower than f_L.

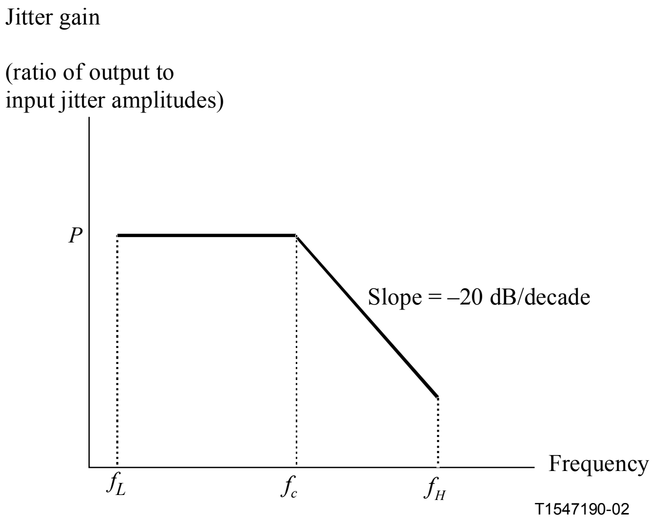

Figure A.1/G.8251 – ODCb jitter transfer

Table A.4/G.8251– ODCb jitter transfer requirement

ODUk level	f_L (Hz)	f_C (kHz)	f_H (kHz)	P (dB)	Input mask
ODU1	10	1	100	0.1	Clause A.6
ODU2	40	4	400	0.1	Clause A.6
ODU3	160	16	1600	0.1	Clause A.6

A.7.2 Jitter transfer for ODCr

The jitter transfer requirements for ODCr are, essentially, the transfer requirements for a 3R regenerator. While the 3R regenerator encompasses all the atomic functions between the OCh/OTUk_A_Sk adaptation function and OCh/OTUk_A_So adaptation function, and includes the wideband clock recovery circuit in the OCh/OTUk_A_Sk, the ODCr (contained in the OTUk/ODUk_A_So and OTUk/ODUk_A_Sk atomic functions) bandwidth is, in practice, significantly narrower than any of the other bandwidths present in the regenerator and therefore determines the transfer characteristics. Because the ODCr bandwidth is much larger than 10 Hz (i.e. the upper limit of the wander region), the regenerators transfer wander without attenuation; there are no explicit wander transfer requirements.

The jitter transfer function of a 3R regenerator is defined as the ratio of the output sinusoidal jitter amplitude to input sinusoidal jitter amplitude, as a function of frequency. The 3R regenerator input is the OCh_AI_D signal at the OCh/OTUk_A_Sk atomic function. The 3R regenerator output is the OCh_AI_D signal at the OCh/OTUk_A_So atomic function. Note that the jitter transfer is not associated with a single atomic function; rather, it is associated with all the atomic functions between and including the OCh/OTUk adaptation sink and source functions. Normally, at least part of the 3R regeneration function must occur in the OCh/OTUk_A_Sk function because a clock must be recovered. However, the jitter transfer and jitter tolerance requirements imply the presence of a second, narrower bandwidth phase-locked loop; this phase-locked loop is in the ODCr, contained in the OTUk/ODUk_A_So and OTUk/ODUk_A_Sk atomic functions.

The jitter transfer function of a 3R regenerator shall be under the curve given in Figure A.1 when input sinusoidal jitter up to the masks of Figures 1, 2 and for OTU1, OTU2, and OTU3, respectively, is applied. The parameters of Figure A.1 are given in Table A.5. Note that the parameter f_C may be considered the maximum bandwidth of the 3R regenerator, and the parameter P the maximum gain peaking of the 3R regenerator. The jitter transfer limit is specified between frequencies of f_L and f_H. The jitter transfer limit is not specified for frequencies higher than f_H nor lower than f_L.

Table A.5/G.8251 – ODCr jitter transfer requirement

OTUk level	f_L (kHz)	f_C (kHz)	f_H (MHz)	P (dB)	Input mask
OTU1	2.5	250	20	0.1	Figure 1, Table 2
OTU2	10	1000	80	0.1	Figure 2, Table 3
OTU3	40	4000	320	0.1	Figure 3, Table 4

A.7.3 Jitter transfer for ODCp

The jitter transfer requirements for ODCp are, essentially, the transfer requirements for a CBR (i.e. SDH) demapper (i.e. desynchronizer). The demapper function, including the ODCp, is contained in the ODUkP/CBRx_A_Sk atomic function. The ODCp performs filtering, which is necessary to control the mapping/demapping jitter and wander accumulation over multiple OTN islands.

The 3 dB bandwidth of the desynchronizer shall not exceed 300 Hz. The maximum gain peaking of the desynchronizer shall be 0.1 dB. These requirements apply to all ODUk rates. Additional information, on demapper phase error, is given in Appendix V.

A.8 Transient response

When a CBR client signal is lost and AIS is inserted, or when the CBR client is restored and AIS is removed, the ODUk and OTUk timing must be maintained. This requirement is met automatically for asynchronous mappings because the ODCa is free-running and therefore independent of the client signal clock. However for bit-synchronous mapping, the ODCb takes its timing from the client. Specifically, the client signal timing is recovered by the clock recovery circuit that resides in the OS/CBR_A_Sk atomic function; the output of this clock recovery circuit is input to the ODCb (see Appendix VI for a summary of the atomic functions). Loss of the client signal results in the ODCb either entering free-run or switching to a free-running AIS clock; restoration of the client signal results in the ODCb switching from free-run condition or from a free-running AIS clock to an independent client-signal clock. In addition, there may be a short period between the instant the client input to the clock recovery circuit is lost and the detection of this loss; during this period, the clock recovery circuit output may be off frequency and still be input to the ODCb. In all these cases, ITU-T Rec. G.798 requires that the ODUk clock shall stay within its limits and no frame phase discontinuity shall be introduced.

The maximum possible frequency difference between an SDH client and free-running ODCb or free-running AIS clock is 40 ppm (because the largest possible offset for each signal is ±20 ppm). The above requirements mean that the ODCb must adequately filter a 40 ppm frequency step such that downstream equipment in the OTN, i.e. 3R regenerators, can tolerate the resulting filtered phase transient. Specifically, this means that the phase transient shall not cause buffer overflow in an ODCr that meets the jitter and wander tolerance requirements of A.6.2. In addition, the ODCb must adequately filter the clock recovery circuit output during the short period between the loss of the client input to the clock recovery circuit and the removal of the clock recovery circuit output from the ODCb input.

If:

1) the clock recovery circuit in the OS/CBR_A_So atomic function loses its input and/or the ODCb loses its input and either enters free-run or switches to an AIS clock; or

2) the ODCb recovers from AIS to the output of the clock recovery circuit,

   the ODCb output shall meet the following requirements:

   a) Any initial frequency step shall not exceed 9 ppm.

   b) Any frequency drift rate following the initial frequency step shall not exceed 200 ppm/s.

   c) The total change in frequency shall not exceed 40 ppm.

The ODCb is allowed to lose synchronization for a period up to 600 ms.

Appendix I

Relationship between network interface jitter requirements and input jitter tolerance

I.1 Network interface jitter requirements

For all OTUk bit rates, two network limits are specified in Table 1: one for a wideband measurement filter and one for a highband measurement filter. The general form of this specification is shown in Table I.1 and is applicable to all OTUk rates.

Table I.1/G.8251 – General form for OTUk interface jitter requirements

Measurement filter	Measurement bandwidth	Peak-to-peak amplitude (UIpp)
Wideband	f_1 to f_4	A_2
Highband	f_3 to f_4	A_1

At any OTUk interface, the following output jitter specifications must be met:

1) Timing jitter as measured over a 60-second interval with a band pass filter with a lower cut-off frequency f_1 and a minimum upper cut-off frequency f_4 shall not exceed A_2 Unit Intervals (UI) peak-to-peak.

2) Timing jitter as measured over a 60-second interval with a band pass filter with a lower cut-off frequency f_3 and a minimum upper cut-off frequency f_4 shall not exceed A_1 Unit Intervals (UI) peak-to-peak.

The roll off at lower cut-off frequency, f_1 and f_3, shall be 20 dB/decade. The roll off at the upper cut-off frequency, f_4, shall be –60 dB/decade.

The value of f_1 reflects the narrowest timing circuit cut-off frequency expected in a line system. The timing circuit may time a regenerator's output signal and could be implemented as a Phase-Locked Loop (PLL). Jitter at frequencies higher than the bandwidth of this PLL will be partially absorbed by the PLL's buffer. The portion not absorbed could cause transmission errors due to buffer spill. Jitter at frequencies lower than this bandwidth will simply pass through without affecting transmission performance. The value of f_1 therefore represents the narrowest bandwidth that might be used in this output timing circuit. The value of f_3 is related to the bandwidth of input timing acquisition circuitry. Jitter at frequencies higher than this bandwidth will constitute alignment jitter and will cause an optical power penalty due to its effect on the eye pattern. This high frequency jitter must therefore be limited to the same degree that equipment specifications limit optical power penalty through jitter tolerance.

The value of f_4 reflects reasonable measurement limitations and is specified to establish minimum measurement bandwidth requirements. f_4 is chosen to include all expected, significant alignment jitter. A value between one and two decades beyond the widest expected 3R regenerator 3 dB bandwidth (cut-off frequency) was chosen (see A.7.2).

The values of A_1 and A_2 are directly related to input sinusoidal jitter tolerance. These parameters have built-in margin and are reasonably conservative because:

1) sinusoidal jitter represents worst-case jitter with respect to input jitter tolerance; and
2) accumulated OTN line (OTUk) jitter will not be sinusoidal (instead, it will be noisy).

I.2 Input jitter tolerance of network equipment

The general form of the weighting filters used for measuring output jitter at a network interface given in Table I.1 are reproduced here in Figure I.1. The filter responses are given in Equations (I-1) and (I-2).

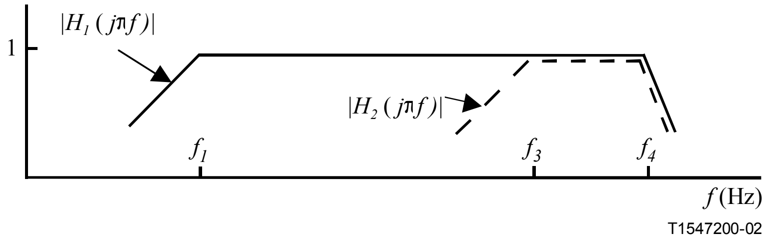

Figure I.1/G.8251 – Weighting filters for measuring network interface output jitter

$$H_1(s) = \frac{s}{s+\omega_1} \cdot \frac{\omega_4^3}{s^3 + 2\omega_4 s^2 + 2\omega_4^2 s + \omega_4^3}$$

$$\left|H_1(2\pi jf)\right|^2 = \frac{f^2}{f^2 + f_1^2} \cdot \frac{f_4^6}{f^6 + f_4^6} \tag{I-1}$$

$$H_2(s) = \frac{s}{s+\omega_2} \cdot \frac{\omega_4^3}{s^3 + 2\omega_4 s^2 + 2\omega_4^2 s + \omega_4^3}$$

$$\left|H_2(2\pi jf)\right|^2 = \frac{f^2}{f^2 + f_2^2} \cdot \frac{f_4^6}{f^6 + f_4^6} \tag{I-2}$$

where:

$$\omega_1 = 2\pi f_1 \qquad \omega_3 = 2\pi f_3 \qquad \omega_4 = 2\pi f_4$$

The first term of the function $H_1(s)$ represents the phase error transfer function $H_e(s)$ of some PLL, and its amplitude of A_2 = 1.5 UIpp represents its phase error tolerance.

Then the corresponding input phase tolerance of the PLL is given by:

$$A_{tol1} = \frac{A_2}{\left|H_1(j2\pi f)\right|} \tag{I-3}$$

Similarly, the input phase tolerance corresponding to $H_2(s)$ and its amplitude of $A_1 = 0.15$ UIpp is given by:

$$A_{tol2} = \frac{A_1}{\left|H_2(j2\pi f)\right|} \tag{I-4}$$

These sinusoidal jitter tolerance masks are illustrated in Figure I.2. If unweighted sinusoidal jitter at a network interface satisfies *both* of these masks, it also satisfies (i.e. lies below) a single mask that is the lower of the two masks for each frequency. Such a combined mask is shown as a dashed curve in Figure I.3.

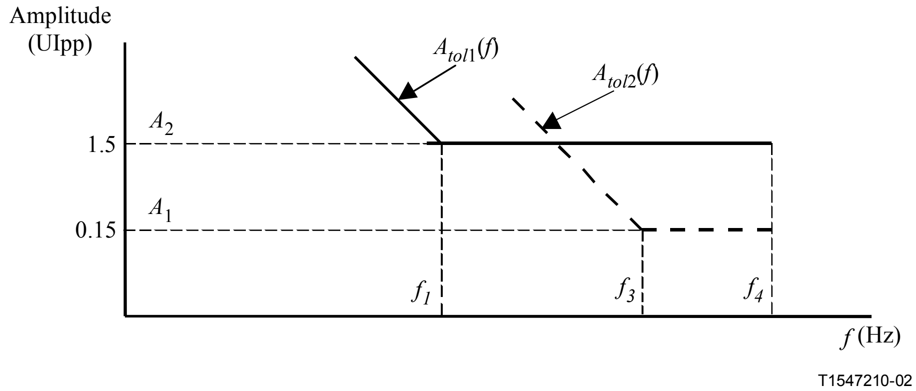

Figure I.2/G.8251 – Upper bounds on sinusoidal jitter amplitude

Figure I.3 compares this combined mask with the OTU1 input jitter sinusoidal tolerance mask. They are the same in the range 500 Hz < f < 20 MHz.

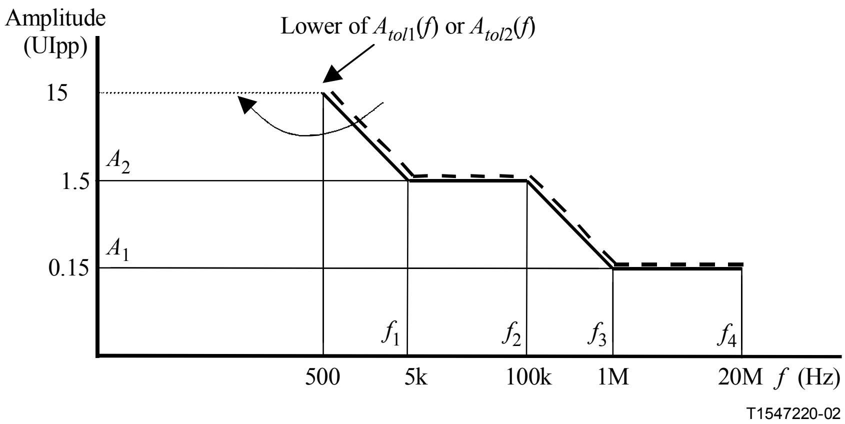

Figure I.3/G.8251 – Upper bound on sinusoidal output jitter at an OTU1 interface [lower of A_{tol1}(f) or A_{tol2}(f)] compared with input jitter/wander tolerance mask

Appendix II

Effect of OTN on the distribution of synchronization via STM-N clients

II.1 Introduction

As stated in clause 1 (Scope) and in 5.2, the OTN physical layer will not be used to transport synchronization. The current standard for the transportation of synchronization over SDH is adequate. However, the introduction of the Optical Transport Network (OTN) changes the position of an STM-N signal in the sense that it can now be a client signal within the OTN layer network. This might affect the synchronization network architecture, since the STM-N signal is currently used as a carrier for synchronization information (next to its payload-carrying capacity). This appendix analyzes possible effects on the synchronization network associated with the introduction of the OTN layer.

II.2 Provisional synchronization reference chain

To analyze the effect of the introduction of the OTN on the synchronization distribution network, the synchronization reference chain from ITU-T Rec. G.803 has been provisionally adapted. The original reference chain contains 1 PRC, 10 SSUs and 60 SECs, under the condition that not more than 20 SECs are concatenated between any pair of SSUs. The provisionally adapted reference model has still 1 PRC and 10 SSUs, but the inter-SSU connections are now presumed to be over the OTN network. At the end of the chain there are 20 SECs (see Figure II.1).

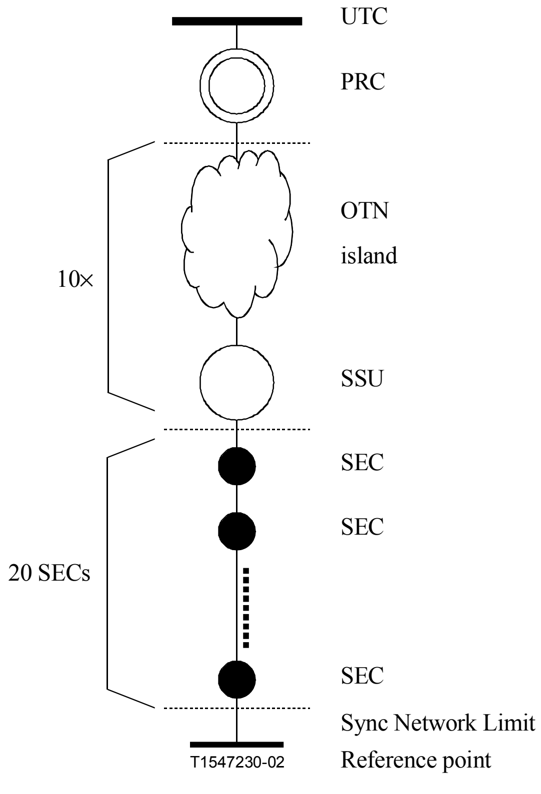

Figure II.1/G.8251 – Adapted synchronization reference chain (Provisional)

The OTN island in this model has to be understood as a conglomerate of OTN equipment that performs mapping of an STM-N into its corresponding ODUk, multiple NEs that perform (de)multiplexing and cross-connecting of ODUk's and transport over optical channels (including optical multiplexing and cross-connecting), and finally demapping of the STM-N.

The composition of each OTN island in the provisional model is assumed to consist of 1 OTN network element that performs the mapping operation and 9 other OTN network elements that perform multiplexing operations of ODUks.

In fact, the distribution of the OTN islands over the adapted synchronization reference model is not important for the long-term wander accumulation. In the model there is one OTN island between each SSU pair, but another distribution is also allowed. For example, five inter-SSU connections may have two OTN islands each while the other interconnections make use of the STM-N physical layer. Also, the number of multiplexing/mapping network elements may be freely re-divided over the OTN islands, to create some "large" and some "small" OTN islands.

In the construction of the adapted synchronization reference chain it is assumed that for the long-term wander accumulation, four SECs equate the effect of one OTN island.

II.3 Synchronization network limit

The network limit that is valid at the end of the synchronization reference chain, as defined in ITU-T Rec. G.803, allows for 5 μs of wander over 24 hours for Option 1 (see ITU-T Rec. G.823) and 1.86 μs over 24 hours for Option 2 (see ITU-T Rec. G.824). It was agreed that in the adapted synchronization reference chain, 10% of the Option 1 budget should be adequate for the combined effect of the OTN islands, i.e. 500 ns (or ~150 bytes at 2.5 Gbit/s).

Since there are 10 OTN islands in the synchronization reference chain, each with 10 mapper/multiplexer NEs a (all assumed to work at the 2.5 Gbit/s rate which represents the worst case), there are 100 of those NEs altogether in the reference chain. Hence, each OTN network element of such type can be allowed 5 ns (or 1.56 bytes at 2.5 Gbit/s) contribution to the long-term wander build-up.

II.4 Variable channel memory

Generically, one can state that the maximum amount of wander that can be accumulated on a path through a network, depends on the maximum amount of propagation delay variation through the network. Propagation delay variations can be caused by elastic buffers that are used in mapping and multiplexing operations. But they can also be caused by fiber, of which the exact propagation delay depends, for example, on temperature. In general, the variable part of the amount of memory in the channel will determine the maximum possible wander. If the propagation delay is $\tau_o \pm \Delta\tau$, the maximum peak-to-peak wander is $2 \cdot \Delta\tau$. (See Figure II.2.)

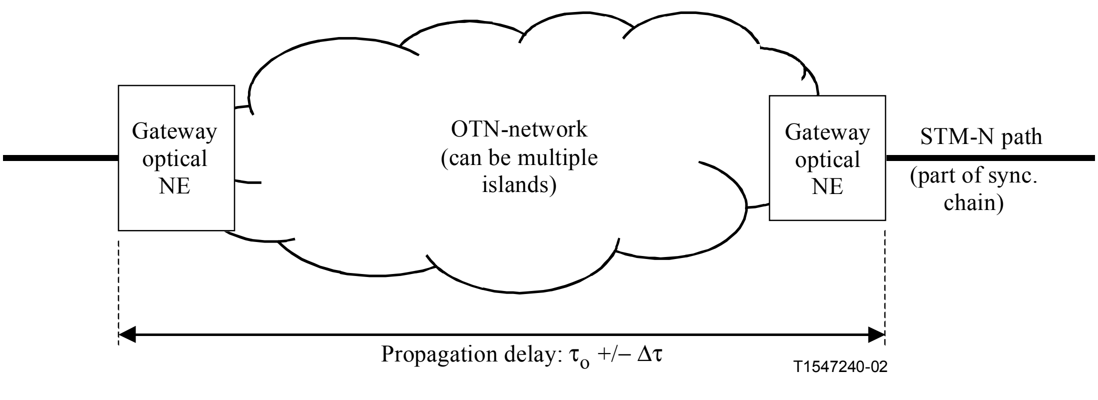

Figure II.2/G.8251 – Variable channel delay

Whether or not the upper wander limit will actually be reached in practical networks depends on a number of factors. The performance of the synchronization of the network is one factor (e.g. this is the main reason why SDH networks require synchronous operation), another factor is the actual design of the elastic buffers. To compute the likelihood of exceeding certain amounts of wander over a certain amount of time with a certain probability requires extensive simulation work, which captures the important details of the elastic-store related processes and the exact network reference model. The disadvantage of this approach is that it is generally not easy to perform these simulations for networks that deviate in some aspects from the reference model. For this reason a worst-case approach based on maximum channel memory variation has been chosen.

II.5 Maximum buffer hysteresis

If each OTN network element is allowed to contribute 5 ns to long-term wander accumulation, the resulting maximum buffer hysteresis is approximately 12.5 UI = 1.5625 bytes for ODU1, 50 UI = 6.25 bytes for ODU2, and 200 UI = 25 bytes for ODU3. Because implementations are often more convenient if they can work with whole numbers of bytes, the ODU1 value is increased to the nearest whole number of bytes, i.e. 2 bytes. The ODU2 value is set to 4 times this, or 8 bytes, and the ODU3 value is set to 16 times this, or 32 bytes. In units of phase time, the buffer hysteresis is approximately 6.4 ns. The total long-term wander budget for the Figure II.1 synchronization reference chain (100 OTN network elements) becomes 640 ns.

ITU-T Rec. G.798 specifies that the maximum allowed buffer hysteresis in alignment functions for mapping and multiplexing operations[1], be restricted to 2 bytes for STM-16, 8 bytes for STM-64, and 32 bytes for STM-256, per OTN NE[2, 3].

The above requirement for elastic store hysteresis per OTN network element should be applied to each possible route of an STM-N or its ODUk envelope through any OTN network element which performs mapping or multiplexing. In case multiple independent paths exist, the requirement should hold for each of these paths individually.

Another assumption made in this appendix is that OTN network elements that do not perform any multiplexing or mapping do not contain elastic buffers and thus do not contribute to the long-term wander accumulation.

Appendix III

Hypothetical Reference Model (HRM) for 3R regenerator jitter accumulation

This appendix describes the Hypothetical Reference Model (HRM) used to obtain the 3R regenerator jitter transfer requirements in A.7.2 and the ODCa, ODCb, and ODCr jitter generation requirements in A.5.1.1. These requirements, together with the HRM, are consistent with the jitter network limits (at an OTUk interface) in 5.1 and the jitter tolerance requirements in 6.1.1 and its subclauses. The details of the 3R regenerator jitter accumulation analyses leading the above requirements and the HRM are given in Appendix IV.

The HRM for 3R regenerator jitter accumulation is given in Figure III.1. The HRM consists of 50 cascaded regenerators, each assumed to meet the jitter generation and transfer requirements of A.5.1.1 and A.7.2, respectively. The 50 3R regenerators are preceded by an ODCa or ODCb, which

---

1 Although desynchronizers and demultiplexers contain elastic stores, these elastic stores do not contribute to the long-term wander accumulation, since the very slow phase variations do not affect the buffer fill.

2 It is assumed that in case both mapping and multiplexing functions are performed on a single STM-N through an OTN NE, that these can be realized with a single alignment operation.

3 Note that this differs from the approach in ITU-T Rec. G.783, where for SDH pointer processors a minimum instead of a maximum amount of buffer hysteresis is prescribed. This is based on the objective of SDH to minimize the number of pointer adjustment events in the network.

is assumed to meet the jitter generation requirements of A.5.1.1. The 50 3R regenerators and ODCa or ODCb, together with the desynchronizer at the demapper, comprise one OTN island. For the case of bit-synchronous mapping, the ODCb is assumed to meet the noise transfer requirement of A.7.1. Under these conditions, the output jitter at the end of the chain of 50 3R regenerators is expected to be within the jitter network limits of Table 1 (see 5.1) and the jitter tolerance masks of Figures 1-3 (Tables 2-4; see 6.1.1.1, 6.1.1.2, and 6.1.1.3, respectively). Note that, for the case of bit-synchronous mapping, it is not necessary to consider jitter accumulation over multiple OTN islands because the jitter accumulation at the egress of an island is effectively filtered by the desynchronizer.

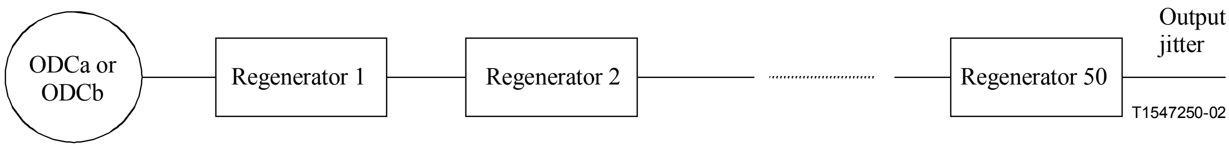

NOTE – For the case of asynchronous mapping, the OTSC has no input (and therefore no jitter on the input). For the case of bit-synchronous mapping, any jitter accumulation in the previous island is filtered by the desynchronizer of that island.

Figure III.1/G.8251 – HRM for 3R regenerator jitter accumulation

Note that other than stating that the 3R regenerators meet the jitter generation requirements of A.5.1.1, no detail is given here on precisely where in each regenerator the noise is generated. For purposes here, it is simply stated that each regenerator meets A.5.1.1 jitter generation requirements in the absence of input jitter. Details of this for two jitter accumulation analyses are given in Appendix IV.

Appendix IV

3R regenerator jitter accumulation analyses

IV.1 Introduction

This appendix describes the details of 3R regenerator jitter accumulation analyses that led to the jitter generation requirements of A.5.1, the jitter transfer requirements of A.7, and the HRM of Appendix III. Two different models were used in respective analyses that were performed independently; however, the models were similar and led to the same results.

Both models were implemented in the frequency domain. Each noise source was modeled via a power spectral density (PSD), which was passed through appropriate filters representing the regenerators. In the first model, the details of the regenerator PLLs were modeled, with noise introduced in various components. In the second model, the noise was modeled via a PSD with an appropriate shape at the regenerator output, and the overall regenerator transfer characteristic (from input to output) was modeled separately. The noise levels were adjusted in both models such that the jitter generation requirements would be satisfied. Jitter generation and output jitter were evaluated using the appropriate measurement filters, which were also modeled with frequency domain transfer functions. The frequency domain models most conveniently produce mean-square jitter as the area under the PSD, and root-mean-square (rms) jitter as the square root of this. Peak-to-peak jitter over 60 s was assumed to be equal to 10 times the rms jitter.[4]

IV.2 Model 1

The regenerator is modeled as a second-order phase-locked loop (PLL) with first-order, proportional-plus-integral (PI) loop filter. Three separate noise sources are assumed to be present, representing phase detector noise, voltage-controlled oscillator (VCO) noise, and thermal noise in the optical receiver just prior to the PLL input. The model is developed for both systematic and random jitter accumulation cases; however, results are given only for random jitter accumulation cases. Jitter accumulation over 3R regenerators is approximately random because the buffer fills in the narrow band phase-locked loops of the successive regenerators (i.e. in the successive ODCrs) are uncorrelated with each other. This is because it is the pattern-dependent jitter that can accumulate systematically, and the pattern-dependent jitter is produced by the clock recovery process in the wideband phase-locked loops. The lack of correlation in the ODCr buffer fills means that read clock pulses with pattern-dependent jitter will time different outgoing bits in successive 3R regenerators. This results in the pattern-dependent jitter is successive regenerators also being uncorrelated.

The following subclauses present the details of the model and give results for selected cases. To minimize the number of simulation cases that must be run, the model is developed in dimensionless form. Two sets of results are given:

1) equivalent 3 dB bandwidth of 8 MHz for the OTU2 case, which is equivalent to the G.783 requirement for STM-64 regenerators; and
2) equivalent 3 dB bandwidth of 1 MHz for the OTU2 case, which is the requirement adopted for this Recommendation in 6.1.3.

The results show that the narrower bandwidth here was necessary in order to meet the jitter network limits of Table 1.

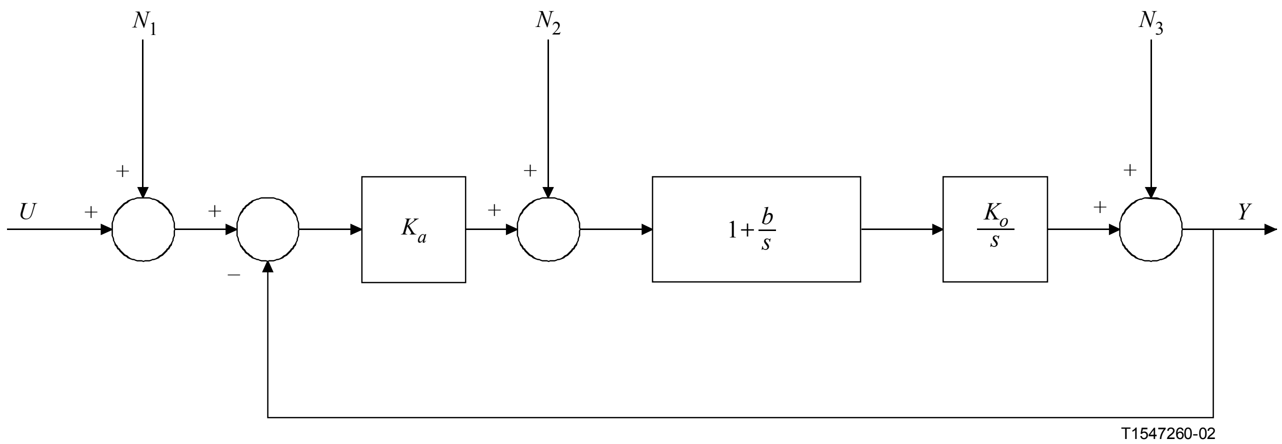

Figure IV.2-1/G.8251 – Regenerator model

---

[4] In defining peak-to-peak jitter or, more generally, the peak-to-peak of any random process, both a measurement interval and a respective quantile (or percentile) should be specified. This is because, if the peak-to-peak measurement is repeated a sufficient number of times (always over the same measurement interval), a distribution of values will be obtained. Here, the measurement interval is taken to be 60 s. The quantile is not specified, but is assumed to be a convenient value consistent with a peak-to-peak to rms ratio of 10. This quantile is expected to be greater than 0.99. If the regenerators can be modeled as linear systems and the noise distribution is Gaussian, then the precise ratio of peak-to-peak to rms jitter is unimportant as long as the generation and output jitter specifications are expressed either both in terms of peak-to-peak jitter or both in terms of rms jitter.

IV.2.1 Model details

The frequency domain analysis follows the methods used in [1] and [2]. The 3R regenerator model is shown in Figure IV.2-1. This is a linear model for a phase-locked loop (PLL). The phase detector gain is K_a, an active loop filter is assumed with transfer function $1+b/s$, and the VCO gain is K_o. $Y(s)$, $U(s)$, $N_1(s)$, $N_2(s)$, and $N_3(s)$, are the Laplace transforms (more precisely, the square root of the respective PSD) of the output, input, optical receiver noise, phase detector noise, and VCO noise, respectively. Then, the transfer functions may be written as follows:

$$
\begin{aligned}
\frac{Y(s)}{N_1(s)} = \frac{Y(s)}{U(s)} \equiv H(s) &= \frac{\frac{K_a K_o}{s}\left(1+\frac{b}{s}\right)}{1+\frac{K_a K_o}{s}\left(1+\frac{b}{s}\right)} = \frac{K_a K_o s + K_a K_o b}{s^2 + K_a K_o s + K_a K_o b} \\
&= \frac{2\varsigma\omega_n s + \omega_n^2}{s^2 + 2\varsigma\omega_n s + \omega_n^2}
\end{aligned}
\quad \text{(IV.2-1)}
$$

$$
\frac{Y(s)}{N_2(s)} = \frac{1}{K_a} H(s) \quad \text{(IV.2-2)}
$$

$$
\begin{aligned}
\frac{Y(s)}{N_3(s)} &= \frac{1}{1+\frac{K_a K_o}{s}\left(1+\frac{b}{s}\right)} = \frac{s^2}{s^2 + K_a K_o s + K_a K_o b} \\
&= \frac{s^2}{s^2 + 2\varsigma\omega_n s + \omega_n^2} = 1 - H(s)
\end{aligned}
\quad \text{(IV.2-3)}
$$

where the undamped natural frequency and damping ration are:

$$
\begin{aligned}
\omega_n &= \sqrt{K_a K_o b} \\
\varsigma &= \frac{1}{2}\sqrt{\frac{K_a K_o}{b}}
\end{aligned}
\quad \text{(IV.2-4)}
$$

Since it will be assumed both N_1 and N_2 are white noise, or white phase modulation (WPM), it will be convenient to combine these into a single equivalent noise source. This may be done as follows:

$$
\begin{aligned}
Y(s) &= H(s)U(s) + H(s)N_1(s) + H(s)N_2(s)/K_a + \left[1 - H(s)\right]N_3(s) \\
&= H(s)U(s) + H(s)N_{12}(s) + H_e(s)N_3(s)
\end{aligned}
\quad \text{(IV.2-5)}
$$

where the equivalent noise source N_{12} is given by:

$$
N_{12}(s) = N_1(s) + N_2(s)/K_a \quad \text{(IV.2-6)}
$$

and the usual notation is used for the phase error transfer function:

$$
H_e(s) \equiv 1 - H(s) \quad \text{(IV.2-7)}
$$

A chain of N 3R regenerators is modeled by assuming the output of the jth regenerator is the input to the $(j+1)$st regenerator, and that the input to the first regenerator in the chain is zero (i.e. the first regenerator is, in essence, a clock and has noise generation but no input jitter). In the following analysis, the cases of systematic and random jitter accumulation are considered separately, using the methodology of [1] and [2]. First, consider the random jitter accumulation case. Here, it is assumed that the corresponding noise sources in all the regenerators have the same magnitude, i.e. the same PSD, but are uncorrelated. The relation between the PSD of the input and output of a single regenerator is [using Equation (IV.2-5)] and setting $s = j\omega$ in the transfer function to obtain the frequency response:

$$S_Y(\omega) = |H(j\omega)|^2 S_U(\omega) + |H(j\omega)|^2 S_{12}(\omega) + |H_e(j\omega)|^2 S_3(\omega) \qquad \text{(IV.2-8)}$$

where $S(\omega)$ with the respective subscript denotes the PSD for the input, output, or respective noise source. Then, for a chain of N 3R regenerators, the PSD of the output phase assuming random jitter accumulation is:

$$\begin{aligned} S_{Nr}(\omega) &= \sum_{j=1}^{N} |H(j\omega)|^{2j} S_{12}(\omega) + \sum_{j=1}^{N} |H_e(j\omega)|^2 |H(j\omega)|^{2j-2} S_3(\omega) \\ &= \frac{|H(jw)|^2 \left[1 - |H(j\omega)|^{2N}\right]}{1 - |H(j\omega)|^2} S_{12}(\omega) + \frac{|H_e(j\omega)|^2 \left[1 - |H(j\omega)|^{2N}\right]}{1 - |H(j\omega)|^2} S_3(\omega) \end{aligned} \qquad \text{(IV.2-9)}$$

For the case of systematic jitter accumulation, it is assumed the corresponding noise sources in the successive regenerators are perfectly correlated, i.e. the N_{12} noise sources in the successive regenerators are perfectly correlated with each other and the N_3 noise sources in the successive regenerators are perfectly correlated with each other. However, it is assumed that an N_{12} noise source and an N_3 noise source are uncorrelated. Then, for a chain of N 3R regenerators, the output phase Y_N at the end of the chain is:

$$\begin{aligned} Y_N(s) &= \sum_{j=1}^{N} H^j(s) N_{12}(s) + \sum_{j=1}^{N} H^{j-1}(s) H_e(s) N_3(s) \\ &= \frac{H(s)\left[1 - H^N(s)\right]}{1 - H(s)} N_{12}(s) + \frac{H_e(s)\left[1 - H^N(s)\right]}{1 - H(s)} S_3(s) \end{aligned} \qquad \text{(IV.2-10)}$$

Then the PSD of the output is related to the noise source PSDs by:

$$S_{Ns}(\omega) = |H(j\omega)|^2 \left| \frac{1 - H^N(j\omega)}{1 - H(j\omega)} \right|^2 S_{12}(\omega) + |H_e(j\omega)|^2 \left| \frac{1 - H^N(j\omega)}{1 - H(j\omega)} \right|^2 S_3(\omega) \qquad \text{(IV.2-11)}$$

The mean square phase at the output of the chain of 3R regenerators is given by the integral of the PSD of Equation (IV.2-9) or (IV.2-11) over all frequencies (from minus infinity to plus infinity). Since the PSD is symmetric about zero, it is convenient to use the one-sided PSD and integrate from zero to infinity. In addition, it is convenient to use the frequency f in Hz rather than ω in rad/s. The usual convention is to define the one-sided PSD as follows:

$$W(f) \equiv 4\pi S(2\pi f) \qquad \text{(IV.2-12)}$$

With this definition, the mean square is equal to the integral of $W(f)$ from zero to infinity. Then, Equation (IV.2-9) for random jitter accumulation becomes:

$$W_{Nr}(f) = \frac{|H(j2\pi f)|^2 \left(1 - |H(j2\pi f)|^{2N}\right)}{1 - |H(j2\pi f)|^2} W_{12}(f) + \frac{|H_e(j2\pi f)|^2 \left(1 - |H(j2\pi f)|^{2N}\right)}{1 - |H(j2\pi f)|^2} W_3(f) \qquad \text{(IV.2-13)}$$

Equation (IV.2-11) for systematic jitter accumulation becomes:

$$W_{Ns}(f) = |H(j2\pi f)|^2 \left| \frac{1 - H^N(j2\pi f)}{1 - H(j2\pi f)} \right|^2 W_{12}(f) + |H_e(j2\pi f)|^2 \left| \frac{1 - H^N(j2\pi f)}{1 - H(j2\pi f)} \right|^2 W_3(f) \qquad \text{(IV.2-14)}$$

Note that Equations (IV.2-13) and (IV.2-14) are the one-sided PSDs for the output phase noise. To obtain the PSDs for output jitter, these equations must be multiplied by the frequency responses of the appropriate jitter measurement filters. The jitter measurement filter consists of a first order high-pass filter followed by a third-order maximally-flat low-pass filter. The frequency response is given by:

$$\left|H_{meas}(j2\pi f)\right|^2 = \frac{f^2}{f^2 + f_{HP}^2} \times \frac{f_{LP}^6}{f^6 + f_{LP}^6} \qquad \text{(IV.2-15)}$$

The cut-off frequencies f_{HP} and f_{LP} depend on the respective rate and whether the jitter is highband or wideband. The specific values are given in Table 1.

Next, Equations (IV.2-13) and (IV.2-14) are rewritten using a dimensionless form of $H(j2\pi f)$. Following [1], define:

$$x = \frac{\omega}{\omega_n} = \frac{f}{f_n} \qquad \text{(IV.2-16)}$$

Then the frequency responses $H(j\omega)$ and $H_e(j\omega)$ may be written [by dividing the numerator and denominator of Equations (IV.2-1) and (IV.2-3) by ω_n^2]:

$$H(x) = \frac{2\varsigma jx + 1}{-x^2 + 2\varsigma jx + 1} \qquad \text{(IV.2-17)}$$

$$H_e(x) = \frac{-x^2}{-x^2 + 2\varsigma jx + 1} \qquad \text{(IV.2-18)}$$

In addition, Equation (IV.2-15) for the jitter measurement filter becomes:

$$H_{meas}(x) = \frac{x^2}{x^2 + (f_{HP}/f_n)^2} \times \frac{(f_{LP}/f_n)^6}{f^6 + (f_{LP}/f_n)^6} \qquad \text{(IV.2-19)}$$

Then Equations (IV.2-13) and (IV.2-14) become:

$$W_{Nr}(x) = \frac{\left|H(x)\right|^2\left(1 - \left|H(x)\right|^{2N}\right)}{1 - \left|H(x)\right|^2} W_{12}(x) + \frac{\left|H_e(x)\right|^2\left(1 - \left|H(x)\right|^{2N}\right)}{1 - \left|H(x)\right|^2} W_3(x) \qquad \text{(IV.2-20)}$$

$$W_{Ns}(x) = \left|H(x)\right|^2 \left|\frac{1 - H^N(x)}{1 - H(x)}\right|^2 W_{12}(x) + \left|H_e(x)\right|^2 \left|\frac{1 - H^N(x)}{1 - H(x)}\right|^2 W_3(x) \qquad \text{(IV.2-21)}$$

(Equations (IV.2-17) to (IV.2-21) are slightly imprecise in the notation because the same symbols for the functions *H* and *W* are used when expressed in terms of *x* rather than *f*; to be more precise, new symbols should have defined, but this would have been cumbersome.)

The advantage of the dimensionless forms Equations (IV.2-17) to (IV.2-21) is that the dependence on the undamped natural frequency or, in essence, the regenerator bandwidth, is gone. The regenerator frequency responses in Equations (IV.2-17) and (IV.2-18) depend only on damping ratio, or, equivalently, on gain peaking. The jitter measurement filter frequency response in Equation (IV.2-19) depends only on the ratio of the high-pass and low-pass filter cut-off frequencies to the regenerator undamped natural frequency or, equivalently, bandwidth. These ratios are the same for the different OTUk rates as long as the values scale with rate; since the gain peaking requirement is also the same for all the rates (0.1 dB), this means that the PSDs may be evaluated once for a given set of ratios, rather than once for each rate.

Finally, the mean square phase and jitter are equal to the appropriate PSD integrated over f from 0 to infinity:

$$\sigma^2 = \int_0^\infty W(f)df = f_n \int_0^\infty W(x)dx \qquad \text{(IV.2-22)}$$

In other words, to obtain the mean square phase or jitter we integrate the dimensionless PSD and multiply by the undamped natural frequency for the respective rate. In addition, and this is most important, it means that the ratio of the mean-square or rms phase or jitter for N regenerators to that for 1 regenerator is independent of the undamped natural frequency and, for the cases here, is the same for all OTUk (because the jitter measurement filter bandwidths and regenerator bandwidths are in the same ratios for all OTUk). This means that the simulations only need to be done once for each set of frequency ratios, rather than once for each value of k and each set of frequency ratios, which reduces the amount of simulation by a factor of 3.

In the examples here, the noise source N_{12} is modeled as white noise:

$$W_{12}(f) = W_{0,12} \qquad \text{(IV.2-23)}$$

In addition, the noise source N_3 represents VCO noise. A model for this is given in [3] and [5]. The VCO PSD is primarily white noise above a frequency f_b, and WFM below f_b:

$$W_3(f) = W_{0,3}\left(1 + \left(\frac{f_b}{f}\right)^2\right) \qquad \text{(IV.2-24)}$$

Equation (IV.2-24) is shown schematically in Figure IV.2-2 (the figure is intended to be a log-log plot; the actual curve would be 3 dB above the breakpoint at frequency f_b. The frequency f_b is given by:

$$f_b = \frac{f_0}{2Q} \qquad \text{(IV.2-25)}$$

where f_0 is the line rate (oscillator frequency) and Q is the quality factor. Inserting Equation (IV.2-25) into Equation (IV.2-24) and dividing numerator and denominator by f_n so that the result may be written in terms of the dimensionless parameter x:

$$W_3(x) = W_{0,3}\left(1 + \left[\frac{(f_0 / f_n)}{2Qx}\right]^2\right) \qquad \text{(IV.2-26)}$$

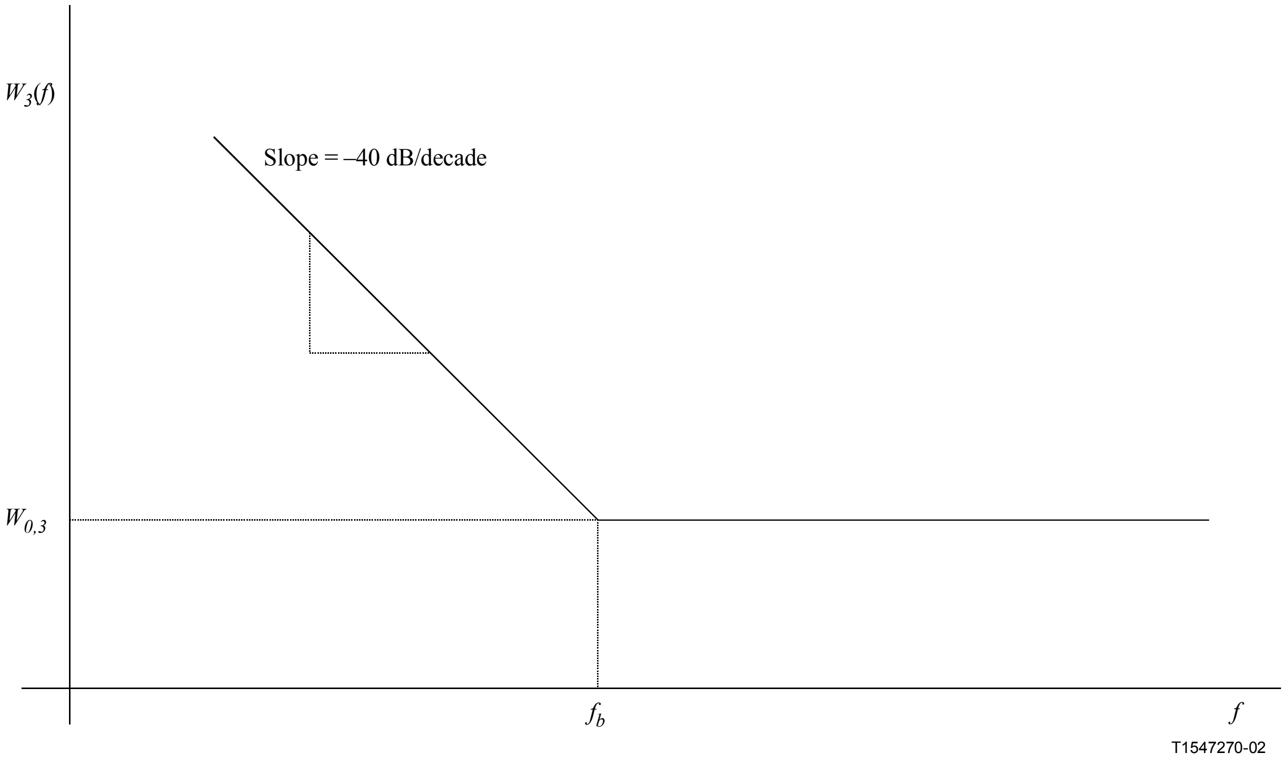

Figure IV.2-2/G.8251 – Schematic of VCO power spectral density

In the examples in the next clause, the ratios of highband and wideband jitter accumulation for N regenerators to the respective jitter for one regenerator, for the N_{12} noise source and for the N_3 noise source separately, are evaluated. This means that the PSD magnitude coefficients $W_{0,12}$ and $W_{0,3}$ cancel on taking the ratio. The results depend only on damping ratio (or, equivalently, gain peaking), ratio of jitter measurement filter cut-off frequencies to undamped natural frequency (or, equivalently, regenerator bandwidth), and, for the N_3 noise source, ratio of line rate to undamped natural frequency and VCO Q-factor. This may be expressed:

$$\frac{\sigma_{12,N}}{\sigma_{12,1}} = F_{12}(a_{LP}, a_{HP}, \varsigma) \tag{IV.2-27}$$

$$\frac{\sigma_{3,N}}{\sigma_{3,1}} = F_3(a_{LP}, a_{HP}, \varsigma, a_0, Q) \tag{IV.2-28}$$

where:

$$\begin{aligned} a_{HP} &= \frac{f_{HP}}{f_n} \\ a_{LP} &= \frac{f_{LP}}{f_n} \\ a_0 &= \frac{f_0}{f_n} \end{aligned} \tag{IV.2-29}$$

The functions F_{12} and F_3 are different for the random and systematic cases; in addition, a_{HP} is different for highband and wideband jitter. But, the functions and the quantities are the same for all three rates (for a given set of frequency ratios) because the various bandwidths are in the same ratios for all three rates.

The relation between undamped natural frequency and 3 dB bandwidth, and between gain peaking and damping ratio, are [see [4] for Equation (IV.2-30) and [3] for Equation (IV.2-31)]:

$$f_{3dB} = f_n \left[2\varsigma^2 + 1 + \sqrt{\left(2\varsigma^2 + 1\right)^2 + 1} \right]^{1/2} \qquad \text{(IV.2-30)}$$

$$H_p = 1 + \frac{1}{4\varsigma^2} \qquad \text{(IV.2-31)}$$

The gain peaking, H_p, in Equation (IV.2-31), is a pure fraction [i.e. the gain peaking in dB is equal to 20 times the log to base 10 of $H_p - 1$ in Equation (IV.2-31)].

A C program was used to evaluate mean-square and rms highband jitter and wideband jitter by numerical integration of the filtered PSD. PSDs were evaluated using a frequency step that was always taken to be less than 0.1 times the minimum bandwidth or cut-off frequency (i.e. less than 0.1 times the wideband jitter high-pass filter cut-off frequency). The extent of the PSD was always taken to be more than 10 times the maximum bandwidth or cut-off frequency (i.e. more than 10 times the low-pass jitter filter cut-off frequency). Note that the jitter measurement filter imposes a maximum bandwidth on the system; i.e. the PSD can be integrated to infinite frequency and the result will converge because of the jitter measurement low-pass filter (we truncate the integration at sufficiently high frequency that the contribution above that frequency is negligible, but not such high frequency that the simulation time is prohibitive).

IV.2.2 Model results

Simulations were run for two sets of regenerator bandwidths, corresponding to SDH requirements in ITU-T Rec. G.783 and OTN requirements in this Recommendation. The former have 3 dB bandwidths of 2 MHz, 8 MHz, and (by extrapolation) 32 MHz for STM-16, -64, and -256 respectively. These values were used for OTU1, 2, and 3, respectively. The latter have 3 dB bandwidths of 250 kHz, 1 MHz, 4 MHz for OTU1, 2, and 3, respectively. All the simulation cases assumed random jitter accumulation.

General parameters for each of the sets of cases are summarized in Table IV.2-1 (SDH bandwidth cases) and in Tables IV.2-2a and IV.2-2b (OTN bandwidth cases). For the requirements of this Recommendation, it was necessary to make separate runs for OTU3 wideband jitter accumulation. This is because the OTU3 wideband jitter high-pass measurement filter bandwidth is the same as that for OTU2 (i.e. it does not scale by a factor of 4 relative to OTU2 as the other parameters do). Parameters for the OTU1 and OTU2 simulation cases are given in Table IV.2-2a; parameters for the OTU3 simulation cases are given in Table IV.2-2b. The jitter measurement filter bandwidths are taken from Table 1. Note that damping ratio and undamped natural frequency are related to gain peaking and 3 dB bandwidth by Equations (IV.2-30) and (IV.2-31).

Table IV.2-1/G.8251 – General parameters for the simulation cases based on G.783 regenerator bandwidths (2 MHz, 8 MHz, 32 MHz, for OTU1, 2, and 3, respectively)

Parameter	Value
Gain peaking H_p	1.0115 (0.1 dB)
Damping ratio ζ	4.6465
$f_{HP,wideband} / f_{3dB}$	2.5×10^{-3}
$f_{HP,highband} / f_{3dB}$	0.5
f_{HP} / f_{3dB}	10
f_0 / f_{3dB}	1339
f_{3dB} / f_n	9.4006

Table IV.2-2a/G.8251 – General parameters for the simulation cases based on G.8251 OTU1 and OTU2 regenerator bandwidths (250 kHz and 1 MHz for OTU1 and 2, respectively)

Parameter	Value
Gain peaking H_p	1.0115 (0.1 dB)
Damping ratio ζ	4.6465
$f_{HP,wideband} / f_{3dB}$	2.0×10^{-2}
$f_{HP,highband} / f_{3dB}$	4.0
f_{LP} / f_{3dB}	80
f_0 / f_{3dB}	10710
f_{3dB} / f_n	9.4006

Table IV.2-2b/G.8251 – General parameters for the simulation cases based on G.8251 OTU3 regenerator bandwidths (4 MHz)

Parameter	Value
Gain peaking H_p	1.0115 (0.1 dB)
Damping ratio ζ	4.6465
$f_{HP,wideband} / f_{3dB}$	5.0×10^{-3}
$f_{HP,highband} / f_{3dB}$	4.0
f_{LP} / f_{3dB}	80
f_0 / f_{3dB}	10755
f_{3dB} / f_n	9.4006

For each set of bandwidths, results are presented for the following cases:

- low-pass filtered noise (e.g. in optical receiver, phase detector, etc.);
- high-pass filtered noise (e.g. in VCO):
  - only WPM (infinite Q);
  - WPM and WFM (Q = 535);
  - WPM and WFM (Q = 100);
  - WPM and WFM (Q = 30).

The three cases with finite Q factor correspond, for OTU2, to the cut-off frequency f_b between WFM and WPM equal to 10 MHz, 53.5 MHz, and 178 MHz. The cases are intended to represent a range of Q factor [the first value was chosen to correspond to a "round" number for cut-off frequency (for the OTU2 case)].

IV.2.2.1 Results for cases based on SDH regenerator bandwidths (ITU-T Rec. G.783)

Figures IV.2-3a and IV.2-3b show highband and wideband jitter accumulation results for the case of low-pass filtered white noise and the case of high-pass filtered white (i.e. WPM only) noise, assuming random jitter accumulation. Figure IV.2-3a shows accumulation over up to 1000 3R regenerators, on a log-log scale. Figure IV.2-3b presents the results on a linear scale; the plot stops at 200 3R regenerators so that results for smaller numbers of regenerators are visible on the scale of the plot.

The results show that:

- wideband jitter accumulates more rapidly than highband jitter;
- noise introduced via a low-pass filter accumulates more rapidly than noise introduced via a high-pass filter.

Regarding the second bullet item, the noise introduced via a high-pass filter hardly accumulates at all until the number of 3R regenerators reaches a few hundred. This lack of accumulation is due to the fact that most of the noise is above the bandwidth of the regenerator; noise introduced in one regenerator is heavily filtered by subsequent regenerators. Note, however, that there is no WFM in the VCO here. The rapid increase after the number of regenerators reaches several hundred is due to the gain peaking of the regenerators.

The results show that after 100 regenerators, wideband and highband jitter have accumulated by factors of approximately 5.5 and 2.0, respectively, for low-pass model white noise, and by factors of less than 1.1 for high-pass model white noise. After 1000 regenerators, wideband and highband jitter have accumulated by factors of approximately 21 000 and 2500, respectively, for low-pass model white noise, and by factors of approximately 400 and 45, respectively, for high-pass model white noise.

Figures IV.2-4a and IV.2-4b show highband and wideband jitter accumulation results for the case of high-pass filtered noise with various amounts of WFM. The relative amount of WFM is indicated via the Q factor; as indicated above, the three cases correspond to cut-off frequencies of 10 MHz (Q = 535), 53.5 MHz (Q = 100), and 178 MHz (Q = 30) for the OTU2 rate [see Equation (IV.2-25)]. A smaller Q indicates a larger relative amount of WFM; Equations (IV.2-24) and (IV.2-25) indicate that reducing Q by a factor increases the WFM component by that factor. As expected, jitter accumulation is larger for the cases with larger WFM component (smaller Q factor). The Q = 535 cases show jitter accumulation approaching about half the accumulation for the low-pass filtered noise case of Figures IV.2-3a and IV.2-3b. In contrast, the Q = 100 and Q = 30 cases show larger accumulation that is very close to that of the low-pass filtered noise case of Figures IV.2-3a and IV.2-3b, for both highband and wideband jitter. This agreement between the low-pass and high-pass model results is due to the fact that, for this range of Q factor (i.e.

below 100) and for the ratios of regenerator to measurement filter bandwidths used here, the result of passing WFM through a high-pass filter gives similar noise to that of passing WPM through a low-pass filter.

Note also that the jitter accumulation for the Q = 100 and Q = 30 cases is very similar. This is because, for both of these cases the frequency f_b is sufficiently above the regenerator bandwidth that the WFM contribution dominates. To see this, note that f_0/f_{3dB} is 1339 (Table IV.2-1), which is sufficiently large compared to the Q factor for these cases (30 and 100). Note that no claim is being made that absolute jitter accumulation is the same in both these cases; the results in Figures IV.2-4a and IV.2-4b are for relative jitter accumulation (jitter out of the jth regenerator divided by jitter out of the first regenerator, and it is this quantity that is the same for both cases.

The results so far show how rapidly highband and wideband jitter accumulate for various noise models. However, it is also of interest to know whether, for a given model, the respective highband or wideband jitter generation limit is more stringent. To determine this, the ratio of wideband to highband jitter generation for a single regenerator, for each model is needed (assuming the same noise source for highband and wideband jitter generation). The ratios are given in Table IV.2-3.

Table IV.2-3/G.8251 – Ratio of wideband to highband rms jitter generation, for one 3R regenerator (SDH 3 dB bandwidths)

Case	Ratio
Low-pass filtered noise	1.2500
High-pass filtered noise, no WFM	1.0136
High-pass filtered noise, with WFM (Q = 535)	1.0502
High-pass filtered noise, with WFM (Q = 100)	1.2078
High-pass filtered noise, with WFM (Q = 30)	1.2400

The ratios indicate that, for the high-pass noise models, wideband jitter generation is not appreciably larger than highband jitter generation. Even for the low-pass noise model, the former is only 25% larger than the latter. These ratios are considerably less than the factor of 3 difference between the wideband and highband jitter generation requirements (0.3 UIpp versus 0.1 UIpp for wideband and highband, respectively; see Table 5).

The results (Figures IV.2-3, IV.2-4, and Table IV.2-3) may now be used to assess whether the jitter network limits of Table 1 can be satisfied for a reference chain of 50 3R regenerators, assuming the regenerators satisfy the SDH requirements of ITU-T Rec. G.783 (and the answer is that the network limits *cannot* be satisfied in this case). Figure IV.2-3b shows that, for low-pass WPM noise, the highband jitter accumulation reaches a factor of 1.5 after approximately 10 regenerators, and is between 1.5 and 2.0 after 50 regenerators. Figure IV.2-4b shows that, for high-pass noise with Q = 30 or 100, the highband jitter accumulation reaches a factor of 1.5 after approximately 10 and 15 regenerators, respectively, and is between 1.5 and 2.0 after 50 regenerators. Since the ratio of the highband jitter network limit to highband jitter generation requirement is 1.5 (i.e. 0.15/0.1), it is seen that a reference chain of regenerators, each of which meet the jitter generation requirements and has low or moderate Q factor, will not meet the jitter network limit. In fact, the network limit will be exceeded after approximately 10 or 11 regenerators. It is only in the high Q factor cases (Q = 535, or the high-pass WPM case, which corresponds to $Q \to \infty$) where the network limit can be met after 50 regenerators; for these cases there is almost no highband jitter accumulation. Note that for the Q = 535 case, the wideband jitter accumulation after 50 regenerators is approximately a factor of 1.9. This meets the wideband jitter network limit, as the ratio of the network limit to generation requirement is 5 (i.e. 1.5/0.3).

In a case where both low-pass and high-pass (VCO) noise are present, it is, in principle, necessary to know the relative amount of each. This plus the simulation results that gave rise to Figures IV.2-3 and IV.2-4 could be used to construct similar curves for the combined case. However, the above results do show that if *Q* factor is sufficiently small (i.e. less than approximately 100, and certainly for values around 30), the low-pass and high-pass noise models give similar results for *relative* jitter accumulation. For these cases, it is not necessary to perform separate simulations of high-pass and low-pass filtered noise, nor is it necessary to know the relative amount of each noise type; instead, it is necessary only to know the total noise generation (and regenerator bandwidth and gain peaking) to determine the jitter accumulation.

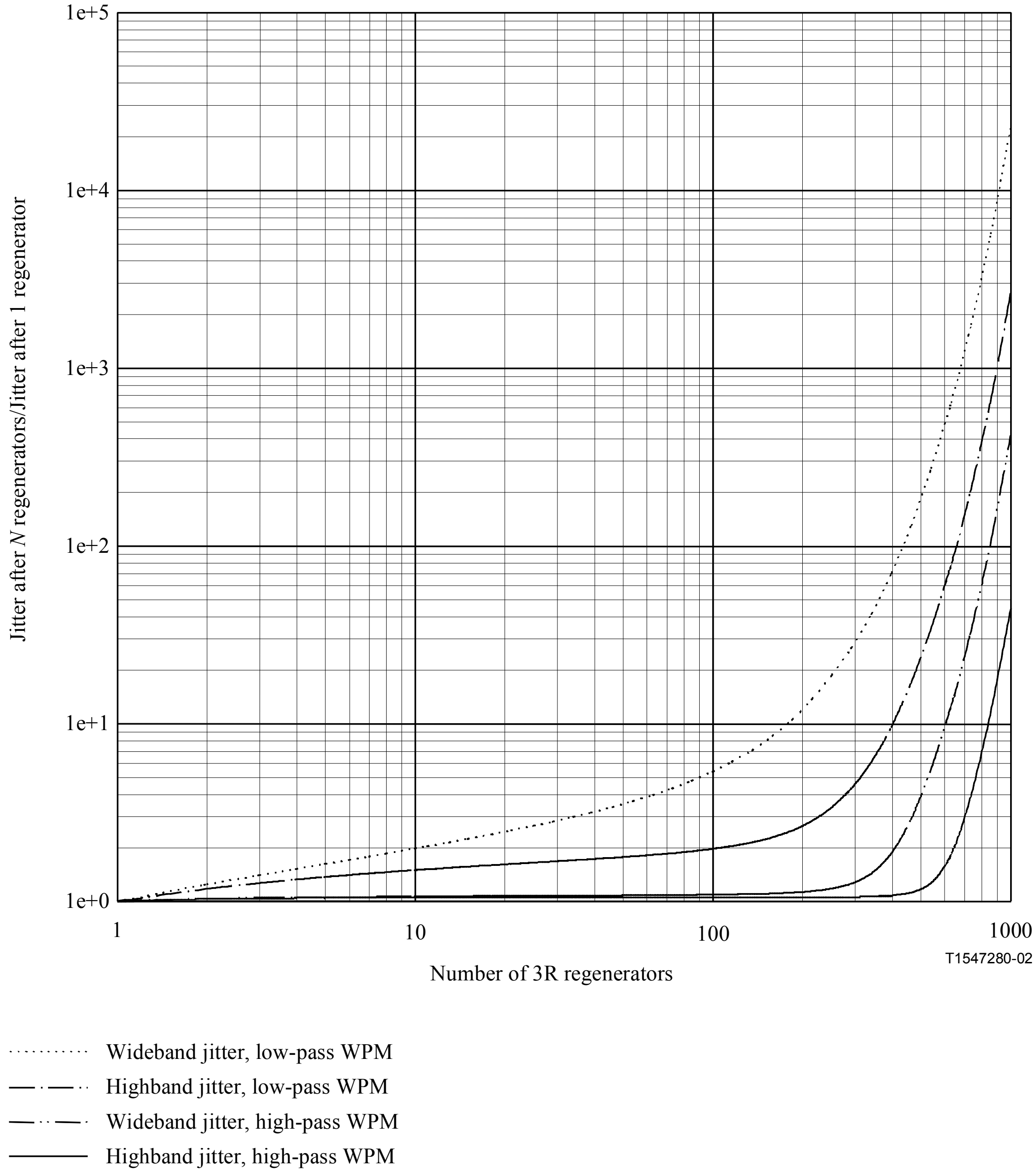

NOTE – Assumptions are: 3R regenerator bandwidths meet G.783 (SDH) requirements, random jitter accumulation, no WFM in VCO (high-pass) noise cases. Log-log plot.

Figure IV.2-3a/G.8251 – Relative increase in jitter over N 3R regenerators

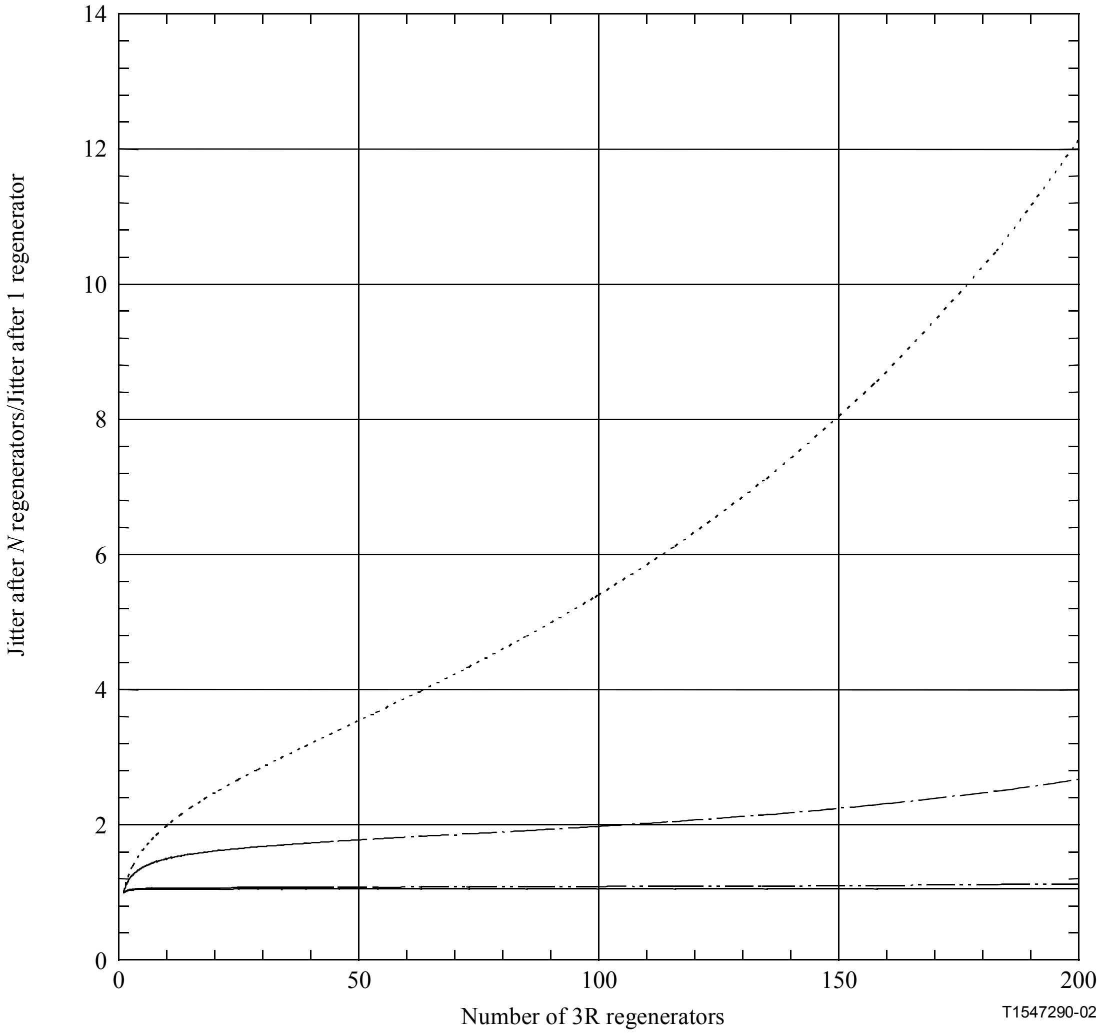

·········· Wideband jitter, low-pass WPM

—·—·· Highband jitter, low-pass WPM

—··— Wideband jitter, high-pass WPM

——— Highband jitter, high-pass WPM

NOTE – Assumptions are: 3R regenerator bandwidths meet G.783 (SDH) requirements, random jitter accumulation, no WFM in VCO (high-pass) noise cases. Linear plot.

Figure IV.2-3b/G.8251 – Relative increase in jitter over *N* 3R regenerators

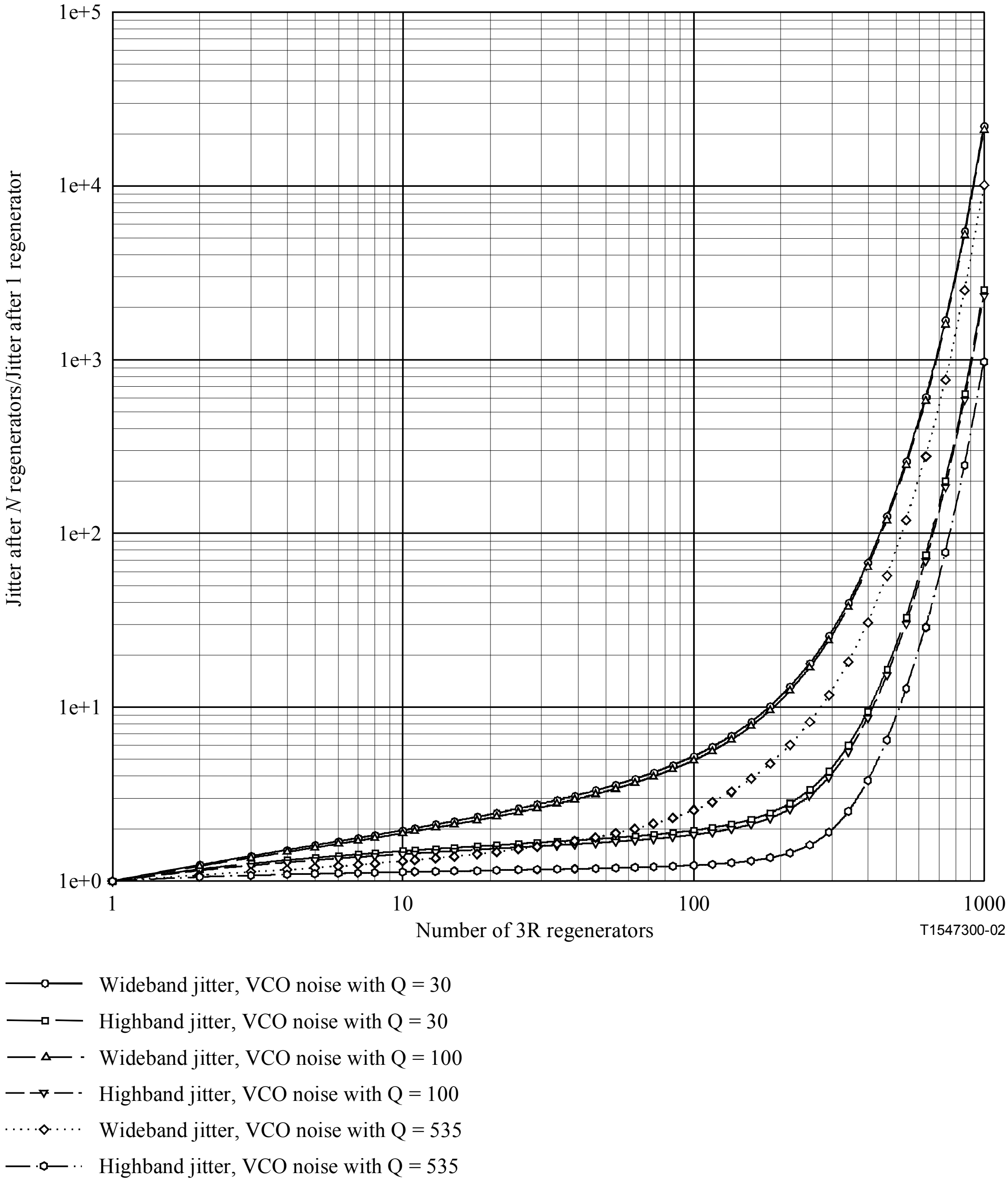

NOTE – Assumptions are: 3R regenerator bandwidths meet G.783 (SDH) requirements, random jitter accumulation, VCO (high-pass) noise with WFM and WPM and indicated *Q*-factor. Log-log plot.

Figure IV.2-4a/G.8251 – Relative increase in jitter over *N* 3R regenerators

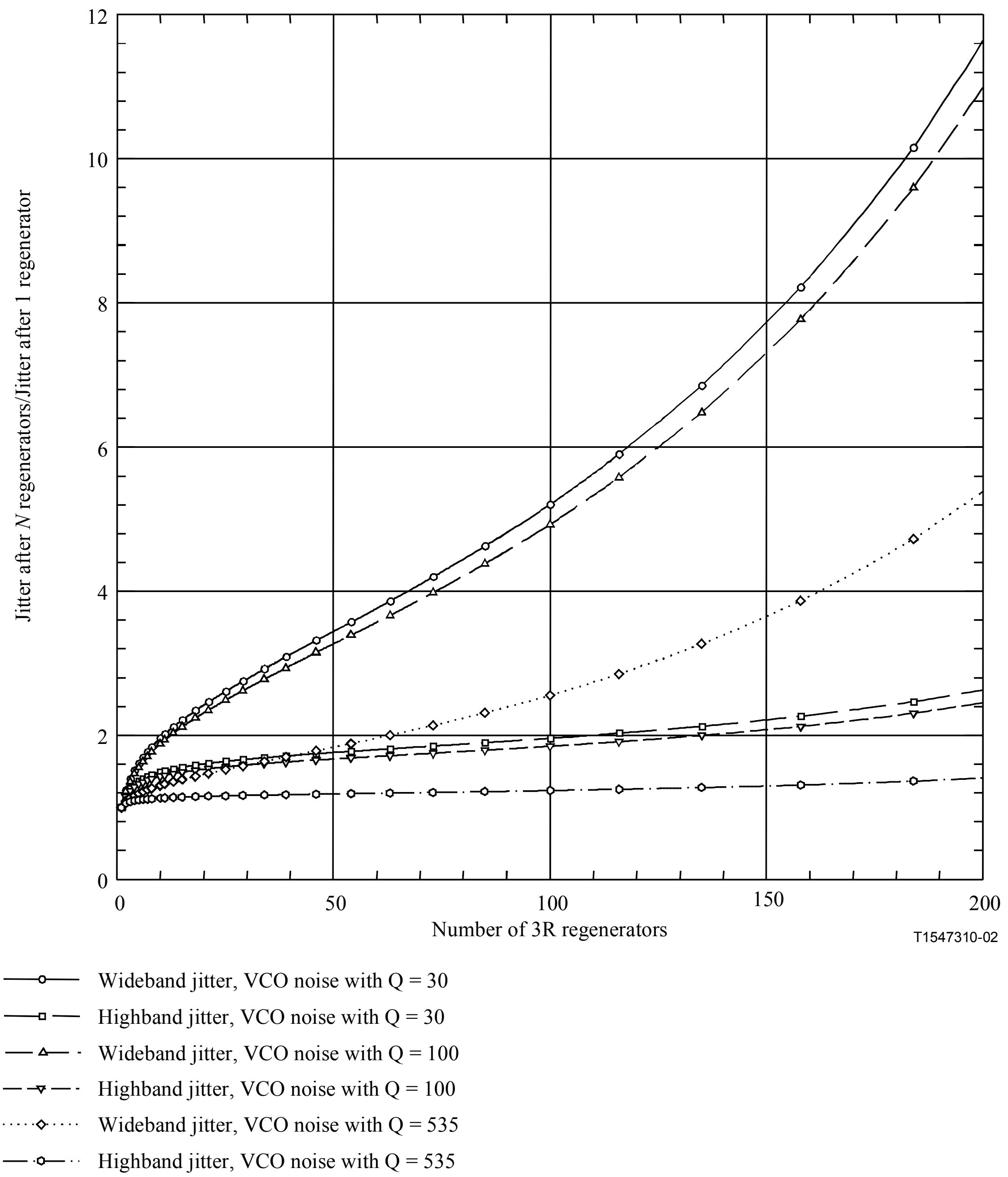

NOTE – Assumptions are: 3R regenerator bandwidths meet G.783 (SDH) requirements, random jitter accumulation, VCO (high-pass) noise with WFM and WPM and indicated *Q*-factor. Linear plot.

Figure IV.2-4b/G.8251 – Relative increase in jitter over *N* 3R regenerators

IV.2.2.2 Results for cases based on OTN 3R regenerator bandwidths (in this Recommendation): Highband jitter for OTU1, OTU2, and OTU3; Wideband jitter for OTU1 and OTU2

Figures IV.2-5 and IV.2-6 (parts a and b for each figure) show wideband jitter results for OTU1 and OTU2 3R regenerators and highband jitter results for OTU1, OTU2, and OTU3 3R regenerators. The 3 dB bandwidths are narrower than the corresponding SDH regenerator bandwidths by a factor of 8. Figures IV.2-5a and IV.2-5b show highband and wideband jitter accumulation results for the case of low-pass filtered white noise and the case of high-pass filtered white (i.e. WPM only) noise, assuming systematic jitter accumulation. Figures IV.2-6a and IV.2-6b show highband and wideband jitter accumulation results for the case of high-pass filtered noise with various amounts of WFM. As with the previous cases, based on SDH regenerator bandwidths, the relative amount of WFM is indicated via the Q factor; the Q factor values used here were the same as in the SDH cases (Q = 30, 100, 535). A smaller Q indicates a larger relative amount of WFM.

Table IV.2-4 shows the ratio of wideband to highband jitter generation for a single regenerator, for each model (assuming the same noise source for highband and wideband jitter generation). Comparing with the results in Table IV.2-3 for SDH bandwidths, it is seen that the ratio of wideband to highband jitter accumulation is larger here. In addition, the degree to which this ratio is larger here is greater for cases where there is a larger portion of noise in the low frequency part of the spectrum. For the low-pass filtered noise case, this is due to the fact that more noise is filtered out in the highband jitter measurement than in the wideband jitter measurement, and the relative amount of noise remaining after filtering in the wideband measurement, relative to the highband measurement, is larger as the regenerator bandwidth is made narrower. For high-pass filtered noise models, the effect is the same as in the low-pass filtered noise model as the Q factor decreases, because for smaller Q factor the noise generation at low frequencies looks more like the low-pass filtered noise model.

Table IV.2-4/G.8251 – Ratio of wideband to highband rms jitter generation, for one OTU1 or OTU2 3R regenerator (OTN 3 dB bandwidths from Table A.4)

Case	Ratio
Low-pass filtered noise	2.2725
High-pass filtered noise, no WFM	1.0308
High-pass filtered noise, with WFM (Q = 535)	1.4862
High-pass filtered noise, with WFM (Q = 100)	2.1927
High-pass filtered noise, with WFM (Q = 30)	2.2605

The jitter accumulation results are qualitatively similar to those for the corresponding SDH cases, except in general there is less jitter accumulation. For example, after 100 regenerators the wideband jitter accumulates by a factor of approximately 5 for the case of low-pass filtered noise (Figure IV.2-5b) and by factors of approximately 4.8, 4.8, and 4 for the case of high-pass filtered noise with Q = 30, 100, and 535, respectively. The corresponding jitter accumulation factors for the SDH regenerator bandwidth cases are 5.5, 5.2, 5, and 2.6, respectively. Note that the only one of these cases where there is less SDH jitter accumulation is the high-pass filtered noise with Q = 535 case. As in the SDH regenerator bandwidth cases, the jitter accumulation for the Q = 100 and Q = 30 cases is very similar.

The results (Figures IV.2-5, IV.2-6, and Table IV.2-4) may now be used to assess whether the OTU1 and OTU2 jitter network limits of Table 1 can be satisfied for a reference chain of 50 3R regenerators, assuming the regenerators satisfy the OTN requirements of Table A.4 (and the answer is that the network limits *can* be satisfied in this case). Figure IV.2-5b shows that, for both low-pass and high-pass WPM noise, the highband jitter accumulation remains very close to a factor of 1 up to 200 regenerators. Figure IV.2-6b shows that, for high-pass noise with Q = 30, 100, or 535, the highband jitter accumulation also remains very close to a factor of 1 up to 200 regenerators. Since the ratio of the highband jitter network limit to highband jitter generation requirement is 1.5 (i.e. 0.15/0.1), it is seen that a reference chain of regenerators, each of which meet the jitter generation requirements, will meet the jitter network limit. The simulation results here show this for 200 regenerators; the highband jitter network limit is certainly met for reference chains of 50 regenerators.

Table IV.2-4 indicates that the largest ratio of wideband to highband jitter generation is approximately 2.27, which occurs for the low-pass filtered noise model. Since the ratio of the wideband to highband jitter generation requirements is 3 (0.3/0.1), it is seen that a regenerator that meets the highband jitter generation requirement will also meet the wideband jitter generation requirement.

Finally, Figures IV.2-5 and IV.2-6 show that the wideband jitter network limits are satisfied for a chain of 50 3R regenerators. The ratio of wideband jitter network limit to wideband jitter generation limit is 5 (1.5/0.3). Figure IV.2-5b shows that wideband jitter increases by factors of 5 and 1, after 100 regenerators, for low-pass filtered WPM and high-pass filtered WPM noise models, respectively. Figure IV.2-6b shows that wideband jitter increases by factors of 4.8, 4.8, and 4, after 100 regenerators, for high-pass filtered noise models with Q = 30, 100, and 535, respectively.

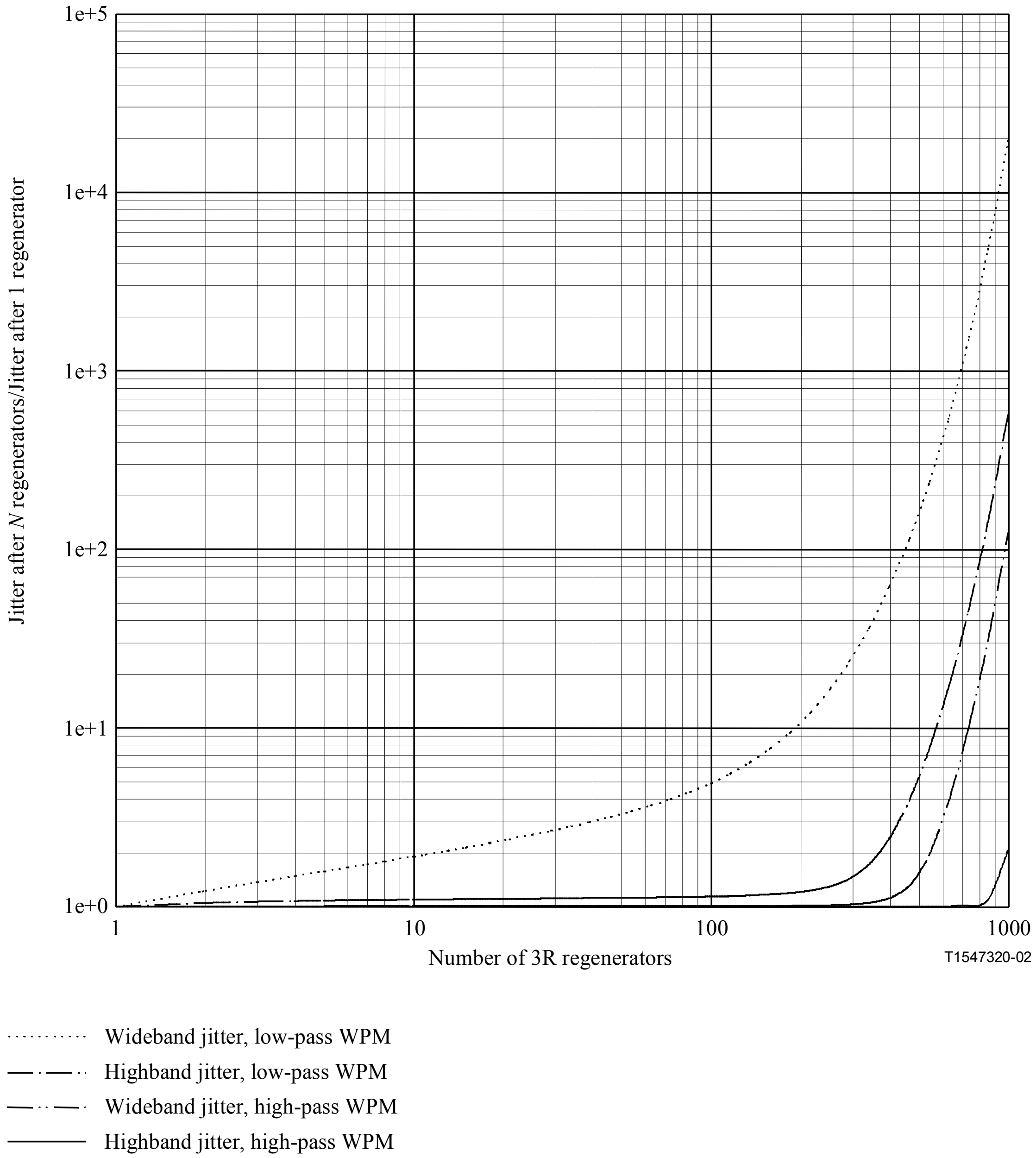

NOTE – Assumptions are: 3R regenerator bandwidths meet G.8251 (OTN) requirements, random jitter accumulation, no WFM in VCO (high-pass) noise cases. Log-log plot.

Figure IV.2-5a/G.8251 – Relative increase in jitter over *N* 3R regenerators

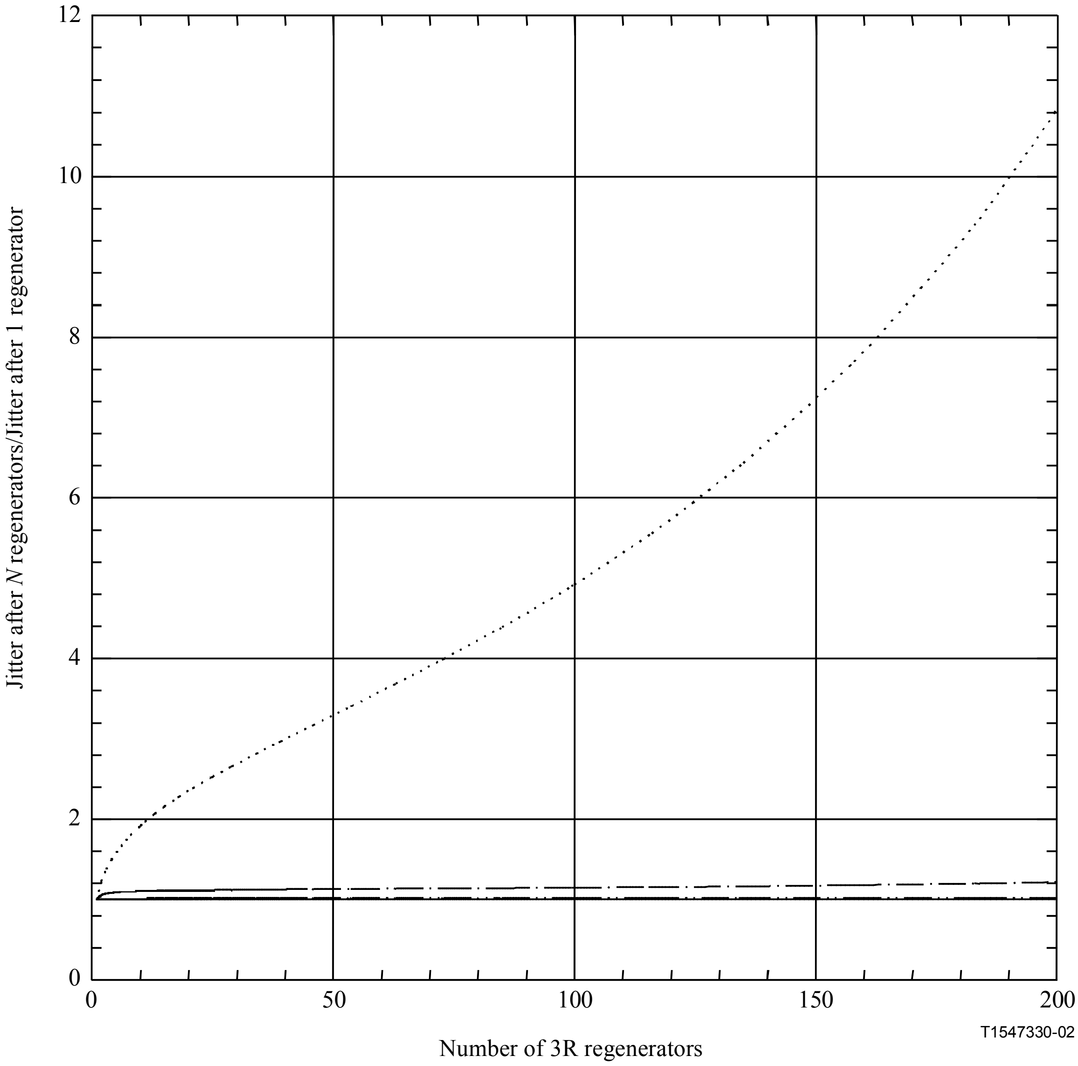

Wideband jitter, low-pass WPM
Highband jitter, low-pass WPM
Wideband jitter, high-pass WPM
Highband jitter, high-pass WPM

NOTE – Assumptions are: 3R regenerator bandwidths meet G.8251 (OTN) requirements, random jitter accumulation, no WFM in VCO (high-pass) noise cases. Linear plot.

Figure IV.2-5b/G.8251 – Relative increase in jitter over *N* 3R regenerators

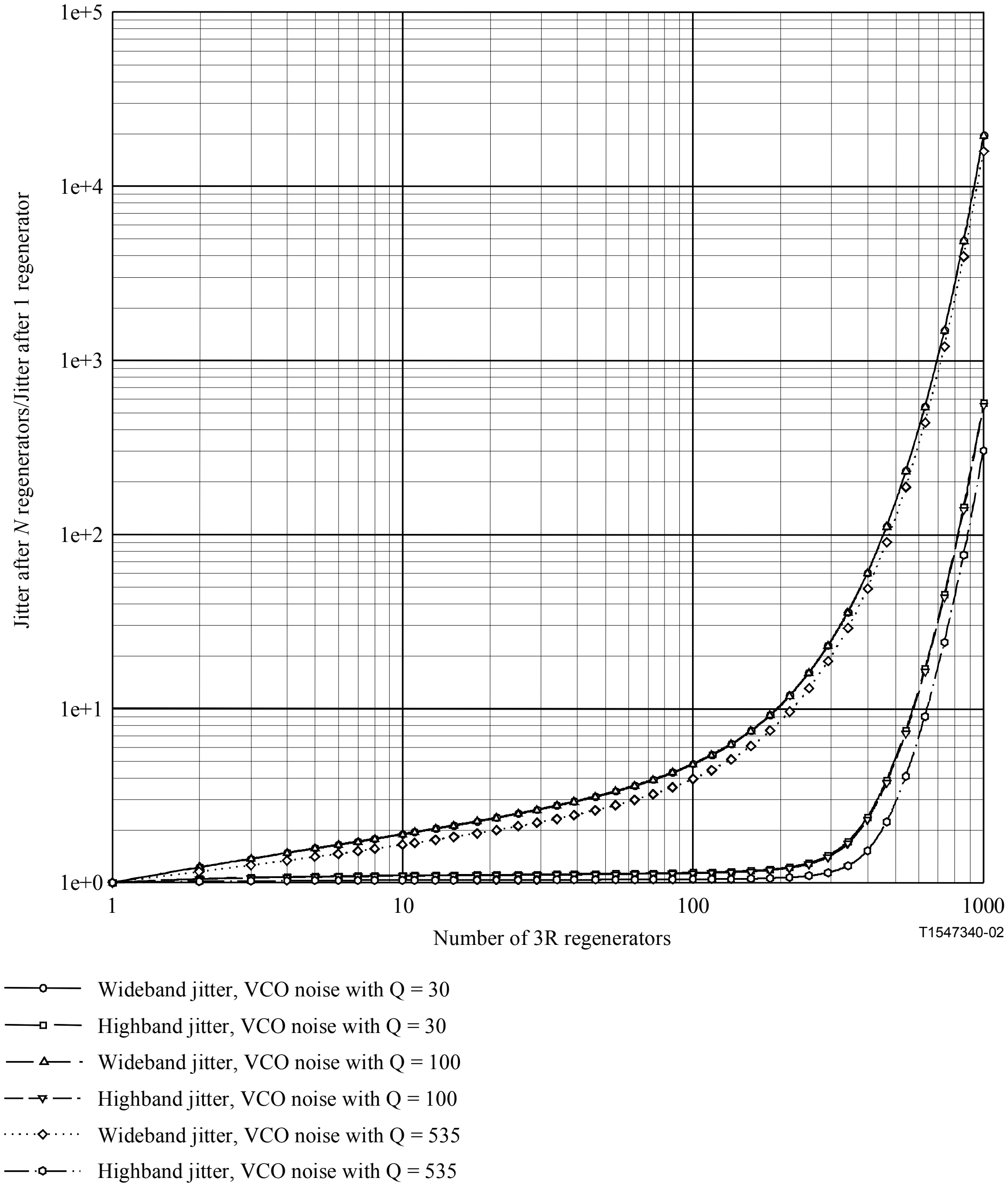

NOTE – Assumptions are: 3R regenerator bandwidths meet G.8251 (OTN) requirements, random jitter accumulation, VCO (high-pass) noise with WFM and WPM and indicated *Q*-factor. Log-log plot.

Figure IV.2-6a/G.8251 – Relative increase in jitter over *N* 3R regenerators

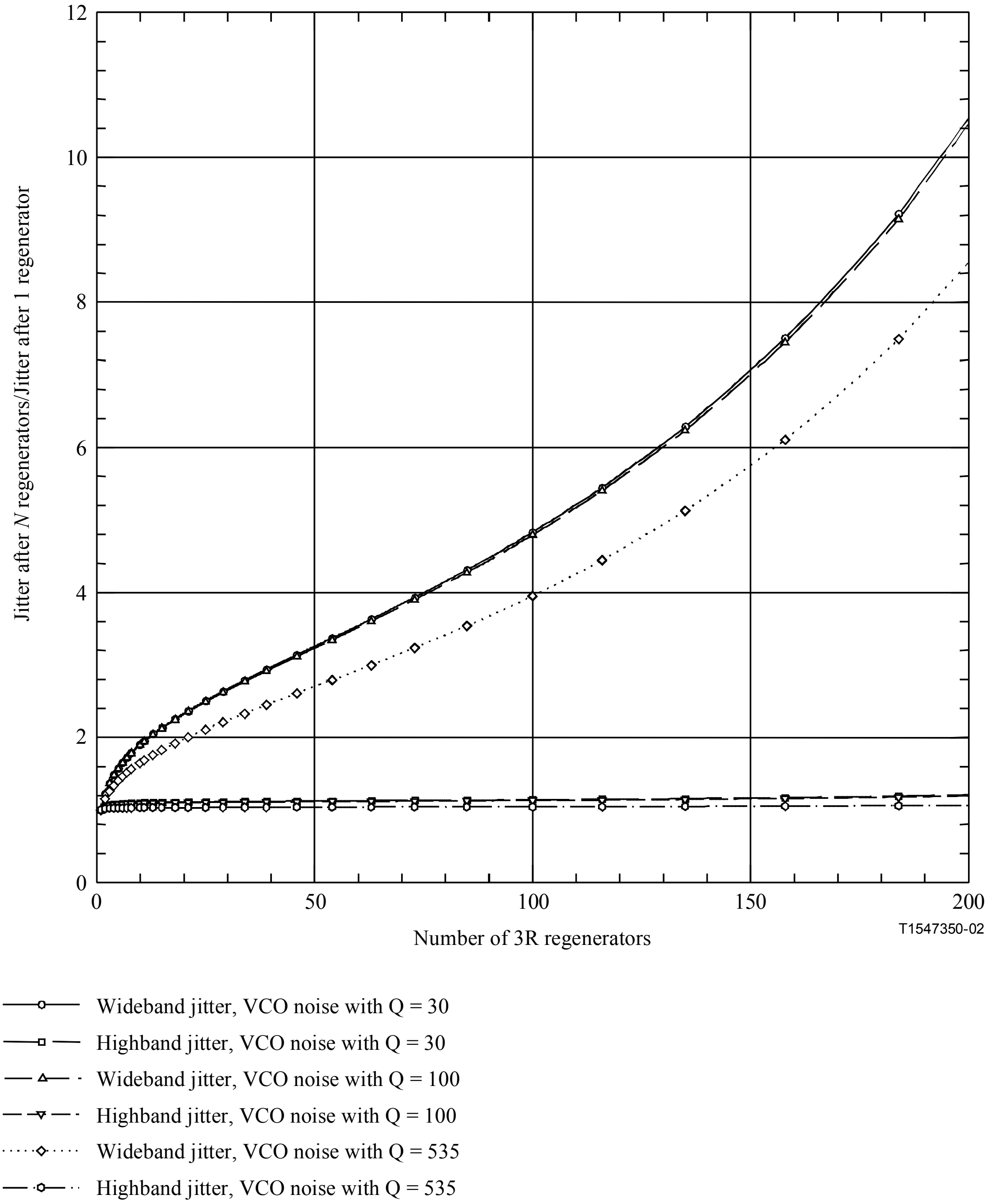

NOTE – Assumptions are: 3R regenerator bandwidths meet G.8251 (OTN) requirements, random jitter accumulation, VCO (high-pass) noise with WFM and WPM and indicated Q-factor. Linear plot.

Figure IV.2-6b/G.8251 – Relative increase in jitter over N 3R regenerators

IV.2.2.3 Results for cases based on OTN 3R regenerator bandwidths (in this Recommendation): Wideband jitter for OTU3

Figures IV.2-7a and IV.2-7b show results for OTU3 wideband jitter accumulation. Comparison with the results above for OTU1 and OTU2 shows almost no change (compare Figure IV.2-7a with the wideband jitter curves in Figures IV.2-5a and IV.2-6a; compare Figure IV.2-7b with the wideband jitter curves in Figures IV.2-5b and IV.2-6b. Table IV.2-4 gives the ratio of wideband to highband rms jitter generation for a single 3R regenerator for OTU1 and OTU2. The corresponding results for OTU3, obtained from the new simulations, are given in Table IV.2-5 (with the results for OTU1 and OTU2 shown in parentheses for comparison). The results for OTU3 are also almost the same as the corresponding results for OTU1 and OTU2.

Table IV.2-5/G.8251 – Ratio of wideband to highband rms jitter generation, for one OTU3 3R regenerator (results for OTU1 and OTU3, from Table IV.2-4, shown in parentheses for comparison)

Case	Ratio
Low-pass filtered noise	2.2898 (compare to 2.2725)
High-pass filtered noise, no WFM	1.0308 (same)
High-pass filtered noise, with WFM (Q = 535)	1.4946 (compare to 1.4862)
High-pass filtered noise, with WFM (Q = 100)	2.2055 (compare to 2.1927)
High-pass filtered noise, with WFM (Q = 30)	2.2734 (compare to 2.2605)

The results may now be used to verify that the OTU3 jitter wideband jitter accumulation is acceptable. Table IV.2-5 shows that the worst ratio of wideband to highband jitter generation (over all the noise models) is approximately 2.29 (versus 2.27 for OTU1 and OTU2). Since the ratio of the wideband to highband jitter generation requirement is 12, it is seen that an OTU3 3R regenerator that meets the highband jitter generation requirement will meet the wideband jitter generation requirement.

Finally, Figure IV.2-7b shows that the largest factor increase in wideband rms jitter after 100 regenerators, among all the noise models, is approximately 5.2, and occurs for low-pass filtered WPM. While this is larger than the ratio for wideband jitter network limit to wideband jitter generation of 5 (6.0/1.2), the network limit is still satisfied assuming the highband jitter requirements are satisfied. This is because, based on the results in Table IV.2-5, meeting the highband jitter generation of 0.1 UIpp means that the wideband jitter generation will only be 0.229 UIpp and not 1.2 UIpp. Therefore, the wideband jitter accumulation will be (5.2)(0.229) = 1.19 UIpp. In any case, note that this is for 100 regenerators; for 50 (as in the Appendix III HRM) the wideband jitter increases by a factor of 3.4. This is well within the ratio of 5.

Therefore, the OTU3 wideband jitter generation requirements are consistent with the OTU3 jitter transfer bandwidth and Appendix III HRM.

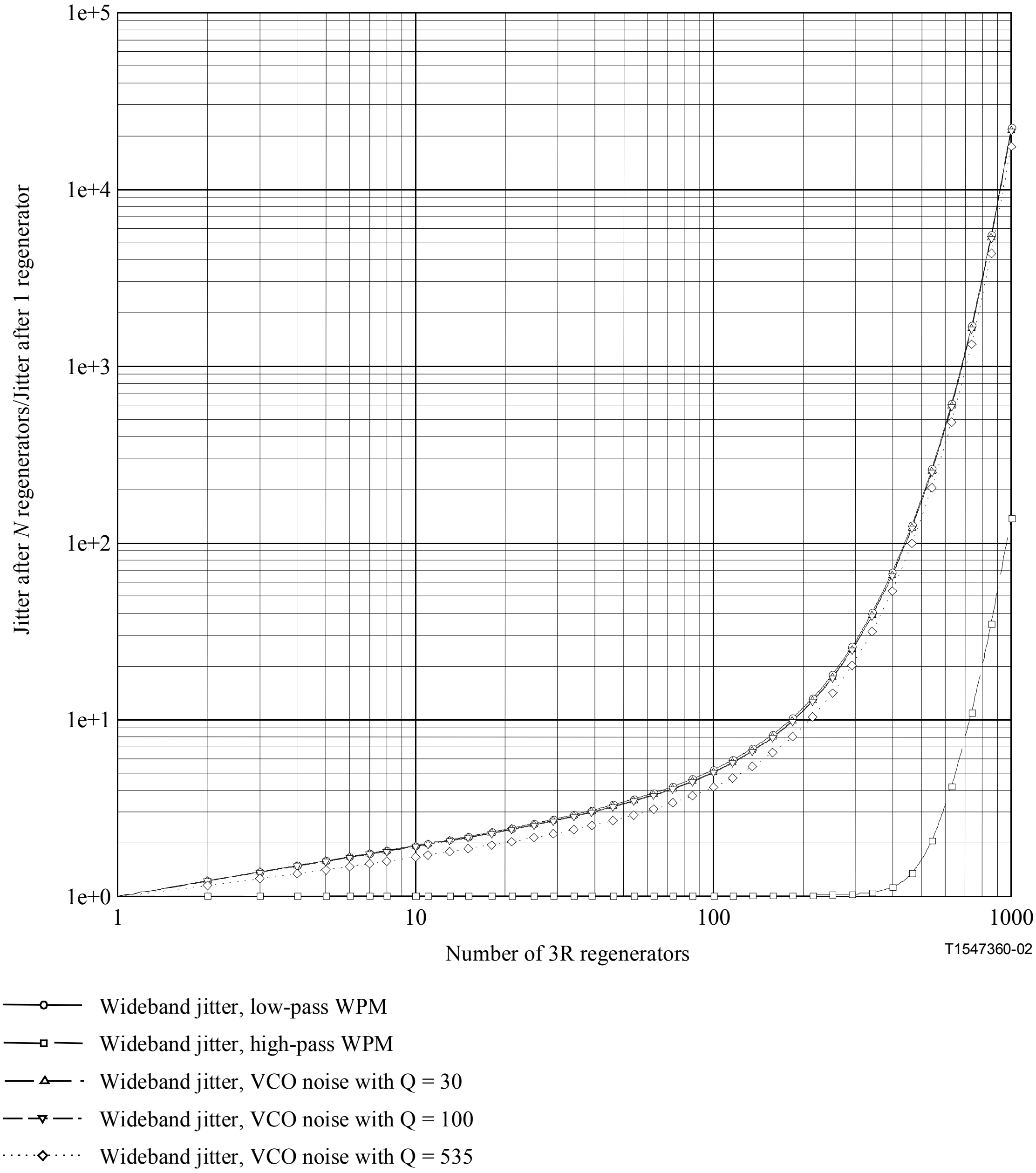

NOTE – Assumptions are: 3R regenerator bandwidths meet G.8251 (OTN) requirements; random jitter accumulation; noise models include: 1) low-pass filtered noise model, 2) VCO (high-pass filtered) noise model with no WFM, and 3) VCO (high-pass filtered) noise models with WFM and WPM and indicated *Q*-factor. Log-log plot.

Figure IV.2-7a/G.8251 – Relative increase in OTU3 wideband jitter over *N* 3R regenerators

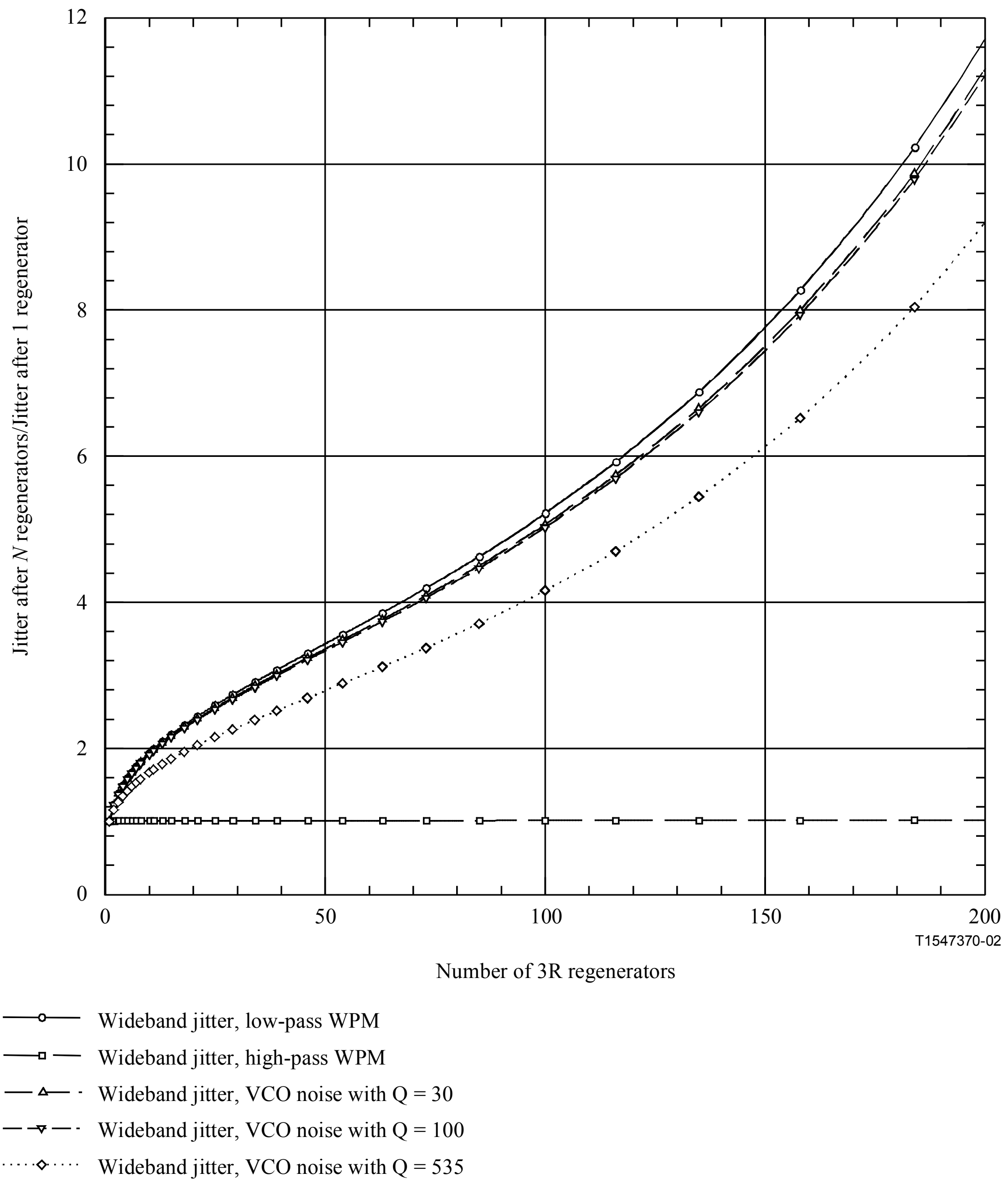

NOTE – Assumptions are: 3R regenerator bandwidths meet G.8251 (OTN) requirements; random jitter accumulation; noise models include: 1) low-pass filtered noise model, 2) VCO (high-pass filtered) noise model with no WFM, and 3) VCO (high-pass filtered) noise models with WFM and WPM and indicated *Q*-factor. Linear plot.

Figure IV.2-7b/G.8251 – Relative increase in OTU3 wideband jitter over *N* 3R regenerators

IV.2.3 References (for Appendix IV)

[1] VARMA (E. L.), WU (J.): Analysis of Jitter Accumulation in a Chain of Digital Regenerators, *Proceedings of IEEE Globecom*, Vol. 2, pp. 653-657,1982.

[2] TRISCHITTA (P. R.) and VARMA (E. L.): Jitter in Digital Transmission Systems, *Artech House*, Norwood, MA, 1989.

[3] WOLAVER (D. H.): Phase-Locked Loop Circuit Design, *Prentice-Hall*, Englewood Cliffs, NJ, 1991.

[4] GARDNER (F. M.): Phaselock Techniques, 2nd Edition, *Wiley*, New York, 1979.

[5] LEESON (D. B.): A Simple Model of Feedback Oscillator Noise Spectrum, *Proc. IEEE*, pp. 329-330, February, 1966.

IV.3 Model 2

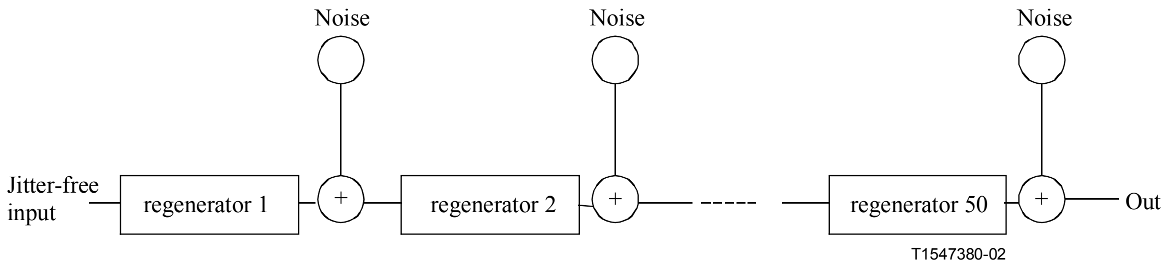

Figure IV.3-1/G.8251 – Schematic of Model 2

IV.3.1 Introduction

A maximum number of 50 regenerators between mapping and subsequent demapping in an OTN island is assumed. A conservative approach in WDM systems using optical amplifiers and dispersion compensating measures leads to a span of more than 300 km between two regeneration operations (total length of 15 000 km). The regenerator model used in previous work based on SDH regenerators is a second-order PLL which filters wideband noise. The wideband noise is assumed as pattern-dependent jitter with constant power spectral density. The 3 dB bandwidth of 8 MHz of the regenerator is the noise shaping filter. The value of the output jitter measured with a band pass filter (4 MHz to 80 MHz) is 0.01 UIrms. Details of the filter are described in ITU-T Rec. G.825.

The same filtering as in ITU-T Rec. G.825 is used here because of the similarity of the STM-64 regenerator and the OTU2 regenerator. The OTU2 bit rate is roughly 7.6% above that of the STM-64. The maximum allowed jitter generation of a STM-64 regenerator in ITU-T Rec. G.783 is given for two combinations of high-pass and low-pass filtering. The jitter value measured in the range between 4 MHz and 80 MHz should not exceed 0.1 UIpp. The value between 20 kHz and 80 MHz should not exceed 0.3 UIpp. This clearly means that roughly 90% of the total noise power could be concentrated in the range below 4 MHz.

Assuming an 8 MHz bandwidth and 0.1 dB gain peaking for such a regenerator would not allow to cascade it in a chain without exceeding the 0.15 UIpp jitter tolerance requirement in ITU-T Rec. G.825. The 0.15 UIpp requirement is the most important requirement. The 4 MHz high-pass filter actually simulates the alignment jitter of a clock recovery with an assumed 4 MHz bandwidth. This alignment jitter also describes the deviation of the sampling time from the static (jitter-free) sampling time inside the receive eye.

If a regenerator is used as in ITU-T Rec. G.783, its bandwidth must be defined. The non-uniform noise distribution is the reason why the bandwidth of the regenerators must be reduced below the value of 8 MHz.

IV.3.2 Structure of the equivalent building blocks in the noise simulation

Each regenerator contains at its output a summation point where the intrinsic jitter is added. The noise spectrum is low-pass filtered White Gaussian Noise. The regenerator jitter transfer function is modelled as a second order PLL with a gain peaking of 0.1 dB. The input of the regenerator must have a clock recovery PLL with corner frequency (i.e. 3 dB bandwidth) greater than 4 MHz (jitter acceptance) which adds some additional filtering to the jitter transfer function. This was not taken into account in the simulation because of the much larger bandwidth compared to the bandwidth of the dominant PLL.

This means that, for the simulation, the bandwidth of the regenerator is modelled only with the (dominant) transfer function of the PLL in the transmit part of the regenerator.

The spectral shaping of the noise source was chosen so that the total noise powers measured after the high-pass – low-pass filter combinations of 20 kHz/80 MHz and 4 MHz/80 MHz differ by a factor of 9. This corresponds to a factor of 3 in rms values and is equivalent to jitter values of 0.3 UIpp and 0.1 UIpp respectively. The noise source does not describe an absolute value. It is used as a normalized reference for the calculation of the accumulation.

The simulation shows that a bandwidth below 1.5 MHz is necessary in order to not exceed the 0.15 UIpp after 50 regenerator operations. Assuming some safety margin a value of 1 MHz is proposed.

The accumulated values for a chain of 50 regenerators with 1 MHz bandwidth, 0.1 dB gain peaking and the maximum allowed noise production according to the values in ITU-T Rec. G.783 are:

– 0.122 UIpp in the upper frequency range;

– 0.815 UIpp in the frequency range from 20 kHz to 80 MHz.

The equivalent proposal for the bandwidth of an OTN regenerator carrying STM-16 client signals is 250 kHz.

IV.4 Jitter generation of regenerators using parallel serial conversion

Regenerators using only one PLL, i.e. the clock recovery, may have requirements which could be contradictory. They have to perform some filtering and their bandwidth has to be large enough to fulfil the jitter tolerance requirement.

The jitter tolerance requires a bandwidth which has to be above the frequency where the first 1/f slope starts. This could lead to a relatively high jitter generation exceeding the maximum allowed value. Generally speaking it is not the purpose of the clock recovery to minimize jitter.

Main requirements for the clock recovery in order to optimise the bit error performance are:

- keeping the sampling time for the data retiming Flipflop independent of the clock frequency at the position of the optimum eye opening (e.g. by using an integrating control loop);
- following the phase modulation of the incoming signal without deviating too much from the ideal sampling time (i.e. jitter tolerance);
- generating a low intrinsic jitter in terms of peak-to-peak values which should not exceed a small portion of the usable eye opening;

  This last bullet point clearly does not contain any requirement regarding the spectral distribution of the intrinsic jitter.

Unlike the measurement of jitter using band-limiting filters, the jitter generated in the clock recovery has to be considered without any filtering because it describes the deviation of the ideal sampling time.

In the case of very high bit rates it could be a problem having a clock recovery which is optimised for error performance while not taking care of the output jitter.

The concept to overcome this difficulty is the use of a serial parallel conversion where the incoming signal normally is converted into bytes. This so-called deserializer often uses a structure of 16 parallel bits.

At this level the frequency where the data processing can be done is reduced by a factor of 16. This allows the use of a phase-locked loop that performs a dejitterizer function with a reduced bandwidth. At the output of such a regenerator the only jitter is that of this PLL and the reasonably low jitter of the PLL performing the multiplexer function and multiplying the clock frequency by a factor of 16.

These concepts allow for higher values of low frequency intrinsic jitter because of the narrower bandwidth of the dejitterizer function. This function filters these phase noise components in regenerators to such a degree that the accumulation in chains, defined in the HRM of Appendix III, does not exceed the network limit.

An example of this is the maximum intrinsic jitter for OTU3 in Table A.2. This can be 1.2 UIpp in the low frequency range.

This value very clearly addresses the possible use of such a triple PLL concept because a value of 1.2 UIpp clearly is not allowed in a one-stage (only clock recovery) regenerator. As shown above it would produce bit errors.

Appendix V

Additional background on demapper (ODCp) phase error and demapper wideband jitter generation requirements

V.1 Introduction

Clause A.7.3 contains the jitter transfer requirements for the demapper clock, i.e. the ODCp. Clause V.2 provides additional information on demapper phase error.

Clause A.5.1.2 contains the jitter generation requirements for the ODCp. It is stated there that one purpose of the ODCp wideband jitter generation requirements is to ensure that the gaps due to fixed overhead in the OTUk frame will not cause excessive output jitter. The wideband jitter generation for ODCp is limited to 1.0 UIpp for STM-16, STM-64, and STM-256 demappers. Clause V.3 provides additional information and background on this requirement.

V.2 Demapper phase error

The demapper (i.e. desynchronizer) is modeled as a second order phase-locked loop (PLL) with 20 dB/decade roll-off. The model is the same as the 3R regenerator Model 1 described in IV.2 and illustrated in Figure IV.2-1; only the numerical values of the parameters are different. Referring to Figure IV.2-1 and Equation (IV.2-1), the transfer function for the desynchronizer is:

$$H(s) = \frac{K_a K_o s + K_a K_o b}{s^2 + K_a K_o s + K_a K_o b} \qquad \text{(V.2-1)}$$

where K_a is the phase detector gain, K_o is the VCO gain, and b is the integral time constant assuming a PI loop filter with transfer function $1+b/s$. The phase error transfer function, i.e. the transfer function between the PLL input and the difference between the PLL output and input, is given by Equation (IV.2-7):

$$H_e(s) \equiv 1 - H(s) = \frac{s^2}{s^2 + K_a K_o s + K_a K_o b} \qquad \text{(V.2-2)}$$

Combining the phase detector gain and VCO gain to obtain an overall proportional time constant τ_p:

$$\tau_p = \frac{1}{K_a K_o} \qquad \text{(V.2-3)}$$

and defining the integral time constant $\tau_i = 1/b$, the phase error transfer function may be rewritten:

$$H_e(s) = \frac{s^2}{s^2 + \frac{s}{\tau_p} + \frac{1}{\tau_p \tau_i}} = \frac{\tau_p \tau_i s^2}{\tau_p \tau_i s^2 + \tau_i s + 1} \quad \text{(V.2-4)}$$

The phase error transfer function may also be written in the canonical form in terms of undamped natural frequency and damping ratio:

$$H_e(s) = \frac{s^2}{s^2 + 2\varsigma\omega_n s + \omega_n^2} \quad \text{(V.2-5)}$$

where:

$$\omega_n = \frac{1}{\sqrt{\tau_p \tau_i}}$$
$$\varsigma = \frac{1}{2}\sqrt{\frac{\tau_i}{\tau_p}} \quad \text{(V.2-6)}$$

Finally, using Equations (IV.2-30) and (IV.2-31), the phase error transfer function may be rewritten in terms of the gain peaking and 3 dB bandwidth. For sufficiently large damping ratio (certainly satisfied by damping ratios on the order of 4 or 5, which is the case here), Equation (IV.2-30) may be approximated by:

$$\omega_{3dB} \cong 2\varsigma\omega_n \quad \text{(V.2-7)}$$

where ω_{3dB} is the 3 dB bandwidth expressed in rad/s. Then:

$$H_e(s) = \frac{s^2}{s^2 + \omega_{3dB} s + \varepsilon\omega_{3dB}^2} \quad \text{(V.2-8)}$$

where the quantity ε is the fractional part of the gain peaking, i.e. see Equation (IV.2-31):

$$\varepsilon \equiv H_p - 1 = \frac{1}{4\varsigma^2} \quad \text{(V.2-9)}$$

The quantity ε is approximately related to the gain peaking in dB by:

$$H_p(dB) = 20\log_{10}(1 + \frac{1}{4\varsigma^2}) \cong 8.6859\ln(1 + \frac{1}{4\varsigma^2}) \cong 8.6859\varepsilon \quad \text{(V.2-10)}$$

Let the input to the ODCp PLL be a frequency drift D (the units of D are fractional frequency offset per second, i.e. s^{-1}). Then the input, expressed as a phase history $u(t)$ in unit intervals (UI), is [the notation $u(t)$, and $U(s)$ for its Laplace transform, are used for the input in V.2 and Figure IV.2-1]:

$$u(t) = \frac{1}{2} D f_0 t^2 \quad \text{(V.2-11)}$$

where f_0 is the input client frequency (i.e. frequency of the client signal at the mapper). The Laplace transform of the input is:

$$U(s) = \frac{D f_0}{s^3} \quad \text{(V.2-12)}$$

The Laplace transform of the phase error is obtained by multiplying the phase error transfer function by the Laplace transform of the phase input; the result is:

$$E(s) \equiv H_e(s)U(s) = \frac{\tau_p \tau_i}{\tau_p \tau_i s^2 + \tau_i s + 1} \times \frac{Df_0}{s} \qquad \text{(V.2-13)}$$

Equation (V.2-13) has the same form as the transfer function for the step response of a damped oscillator; for damping ratio greater than 1 (which is the case here) the oscillator is overdamped and there is no overshoot. In this case, the maximum response, i.e. the maximum phase error, is equal to the steady-state phase error. This is given by:

$$E_{\mathrm{ss}} \equiv \lim_{t \to \infty} e(t) = \lim_{s \to \infty} sE(s) = Df_0 \tau_p \tau_i \qquad \text{(UI)} \qquad \text{(V.2-14)}$$

The units of the steady-state phase error in Equation (V.2-14) are UI. To obtain the result in units of time, this must be divided by the client frequency f_0:

$$E_{ss} = D\tau_p \tau_i \qquad \text{(s)} \qquad \text{(V.2-15)}$$

This may be rewritten in terms of 3 dB bandwidth and damping ratio using Equations (V.2-6) and (V.2-7):

$$E_{ss} = D\frac{4\varsigma^2}{\omega_{3dB}^2} = \frac{D\varsigma^2}{\pi^2 f_{3dB}^2} \qquad \text{(s)} \qquad \text{(V.2-16)}$$

Inserting $D = 10^{-8}$/s, $\zeta = 4.6465$ [which corresponds to 0.1 dB gain peaking; see Equation (IV.2-31)], and $f_{3dB} = 300$ Hz, the steady-state phase error is:

$$E_{ss} = \frac{(10^{-8} s^{-1})(4.6465)^2}{\pi^2 (300\,\text{Hz})^2} = 2.43 \times 10^{-13}\,\text{s} = 0.243\,\text{ps} \qquad \text{(V.2-17)}$$

In Equation (V.2-17), the 3 dB bandwidth and gain peaking just meet the requirements of A.7.3 (300 Hz and 0.1 dB, respectively). In practice, the bandwidth and gain peaking will be somewhat lower. It is seen from Equation (V.2-16) that decreasing the 3 dB bandwidth and gain peaking (i.e. increasing the damping ratio) will cause the steady-state phase error to increase. For example, if the 3 dB bandwidth is 150 Hz and the gain peaking is 0.5% [i.e. approximately 0.043 dB using Equation (V.2-10), which corresponds to a damping ratio of 7.07], the steady-state phase error is:

$$E_{ss} = \frac{(10^{-8} s^{-1})(7.07)^2}{\pi^2 (150\,\text{Hz})^2} = 2.25 \times 10^{-12}\,\text{s} \cong 2.3\,\text{ps} \qquad \text{(V.2-18)}$$

V.3 Demapper wideband jitter generation due to gaps produced by fixed overhead in OTUk frame

The jitter and wander transfer requirements for ODCp given in A.7.3 and Table A.1 ensure that the jitter due to the mapping and demapping of client signals into and out of OPUk, possibly multiple times, will be acceptable (i.e. will satisfy the respective network limits, which are given in ITU-T Rec. G.825 for the case of SDH clients). The ODCp jitter generation requirements given in A.5.1.2 and Table A.3 ensure that any additional jitter produced by the ODCp will be within limits. An ODCp that does not generate any additional jitter and meets the transfer requirements of A.7.3, namely 3 dB bandwidth not exceeding 300 Hz and gain peaking not exceeding 0.1 dB, will meet the requirements of Table A.3. For example, the zero-to-peak wideband jitter due to a single justification when an STM-16 is demapped from an OPU1 is approximately 0.4 UIpp assuming a 300 Hz bandwidth, 0.1 dB gain peaking, and 5 kHz high-pass jitter measurement filter for wideband jitter. The peak-to-peak jitter is therefore twice this, or approximately 0.8 UIpp. This is within the 1.0 UIpp requirement of Table A.3.

The additional margin in the Table A.3 requirements allows for some ODCp jitter generation, while keeping total jitter accumulation acceptable. One possible source of ODCp jitter generation is the jitter due to the gaps caused by the fixed overhead in the OTUk frame. This jitter is considered in this clause, and it is shown that the addition of a suitable filter following the proportional-plus-integral filter in the ODCp phase-locked loop (PLL) can reduce this jitter to a level that is negligible.

As in V.2, the demapper is modeled as a PLL using the model of Figure IV.2-1; however, now an additional filter $G(s)$ is inserted between the loop filter ($1+b/s$) and VCO (K_o/s). The form of $G(s)$ will be specified later. The transfer function, $H(s)$, for the PLL is:

$$H(s) = \frac{\dfrac{K_a K_o}{s}\left(1+\dfrac{b}{s}\right)G(s)}{1+\dfrac{K_a K_o}{s}\left(1+\dfrac{b}{s}\right)G(s)} = \frac{(K_a K_o s + K_a K_o b)G(s)}{s^2 + (K_a K_o s + K_a K_o b)G(s)} \qquad \text{(V.3-1)}$$

where K_a is the phase detector gain, K_o is the VCO gain, and b is the integral time constant assuming a PI loop filter with transfer function $1+b/s$. Defining the proportional time constant as in Equation (V.2-3), the integral time constant $\tau_i = 1/b$, the undamped natural frequency and damping ratio as in Equation (V.2-6), the 3 dB bandwidth as in Equation (V.2-7) (in units of rad/s), and the fractional part of the gain peaking as in Equation (V.2-9), the transfer function may be rewritten:

$$H(s) = \frac{(\omega_{3dB} s + \varepsilon\omega_{3dB}^2)G(s)}{s^2 + (\omega_{3dB} s + \varepsilon\omega_{3dB}^2)G(s)} \qquad \text{(V.3-2)}$$

Setting $s = j\omega$ in Equation (V.3-2) to obtain the frequency response, dividing numerator and denominator by ω_{3dB}^2, and defining the dimensionless quantity $x = \omega/\omega_{3dB} = f/f_{3dB}$ (where $\omega = 2\pi f$ and $\omega_{3dB} = 2\pi f_{3dB}$), produces:

$$H(j\omega) = \frac{(jx+\varepsilon)G(j\omega)}{-x^2 + (jx+\varepsilon)G(j\omega)} \qquad \text{(V.3-3)}$$

Each row of an OTUk, ODUk, and OPUk frame has 3808 bytes of OPUk payload and 272 bytes of OPUk, ODUk, and OTUk overhead (see ITU-T Rec. G.709). The 272 bytes of overhead gives rise to a gap of size (8)(272) UI = 2176 UI. This gap repeats with period equal to one-fourth the OTUk frame period (because the OTUk frame has 4 rows). The result is a sawtooth phase waveform with amplitude of 2176 UI and period equal to the OTUk frame period divided by 4. The worst case is OTU1 (i.e. STM-16 mapped into ODU1), because here the frame period is largest. The remainder of this clause will focus on this case. The resulting sawtooth period is 48.971 μs /4 = 12.243 μs. The frequency of the sawtooth is 81.68 kHz.

An approximate value for the magnitude of the frequency response may be obtained by noting that a Fourier decomposition of the sawtooth consists of a fundamental frequency of 81.68 kHz and harmonics. Since f_{3dB} = 300 Hz, the quantity x is of order 81680/300 = 272 or larger. The quantity ε, which is the fractional part of the gain peaking, is of order 0.1 dB/8.6859 = 0.012 [see Equation (V.2-10)]. Then $x \gg \varepsilon$. In addition, the filter $G(s)$ is a low-pass filter; its magnitude is never much greater than 1 (assuming small gain peaking) and much less than 1 for frequencies above its bandwidth. Finally, note that $x^2 = (272)^2 = 73980 \gg x$. Then the magnitude of the frequency response given in Equation (V.3-3) may be approximated:

$$|H(j\omega)| \cong \frac{|G(j\omega)|}{x} \tag{V.3-4}$$

Consider first the case where the filter $G(s)$ is not present, i.e. $G(s) = 1$. Then the PLL reduces the amplitude of each frequency component of the sawtooth by a factor x. An order of magnitude estimate of the jitter may be obtained by assuming the entire energy of the sawtooth is concentrated in the lowest harmonic and the amplitude is 2176 UIpp. The resulting jitter is 2176 UIpp / 272 = 8 UIpp. A more exact value of 6.3 UI was obtained via time-domain simulation using a sawtooth input. In any case, the jitter is far in excess of the 1.0 UIpp limit of Table A.3.

To reduce the jitter to an acceptable level, the filter $G(s)$ may be taken to be a third-order, low-pass filter with bandwidth of approximately 0.1 times the frequency of the sawtooth, i.e.:

$$G(s) = \left(\frac{a}{s+a}\right)^3 \tag{V.3-5}$$

with $a = 2\pi f_a = 2\pi$ (8200 Hz). Then, again making the approximation that all the energy of the phase waveform is in the lowest harmonic with frequency of 81.68 kHz, the magnitude of the frequency response is approximately:

$$|G(j\omega)| = \left(\frac{f_a}{\sqrt{f^2 + f_a^2}}\right)^3 \approx (0.1)^3 = 0.001 \tag{V.3-6}$$

The order of magnitude estimate of jitter is reduced to 8×10^{-3} UIpp = 8 mUIpp. A more exact value of 6.3×10^{-3} = 6.3 mUIpp was obtained via time-domain simulation using a sawtooth input. In any case, the jitter is now well within the 1.0 UIpp limit of Table A.3.

Appendix VI

OTN atomic functions

VI.1 Introduction

Figure VI.1 summarizes the atomic functions used for OTN timing. Table A.1 indicates the relationships between the ODCa, ODCb, ODCr, and ODCp and these atomic functions.

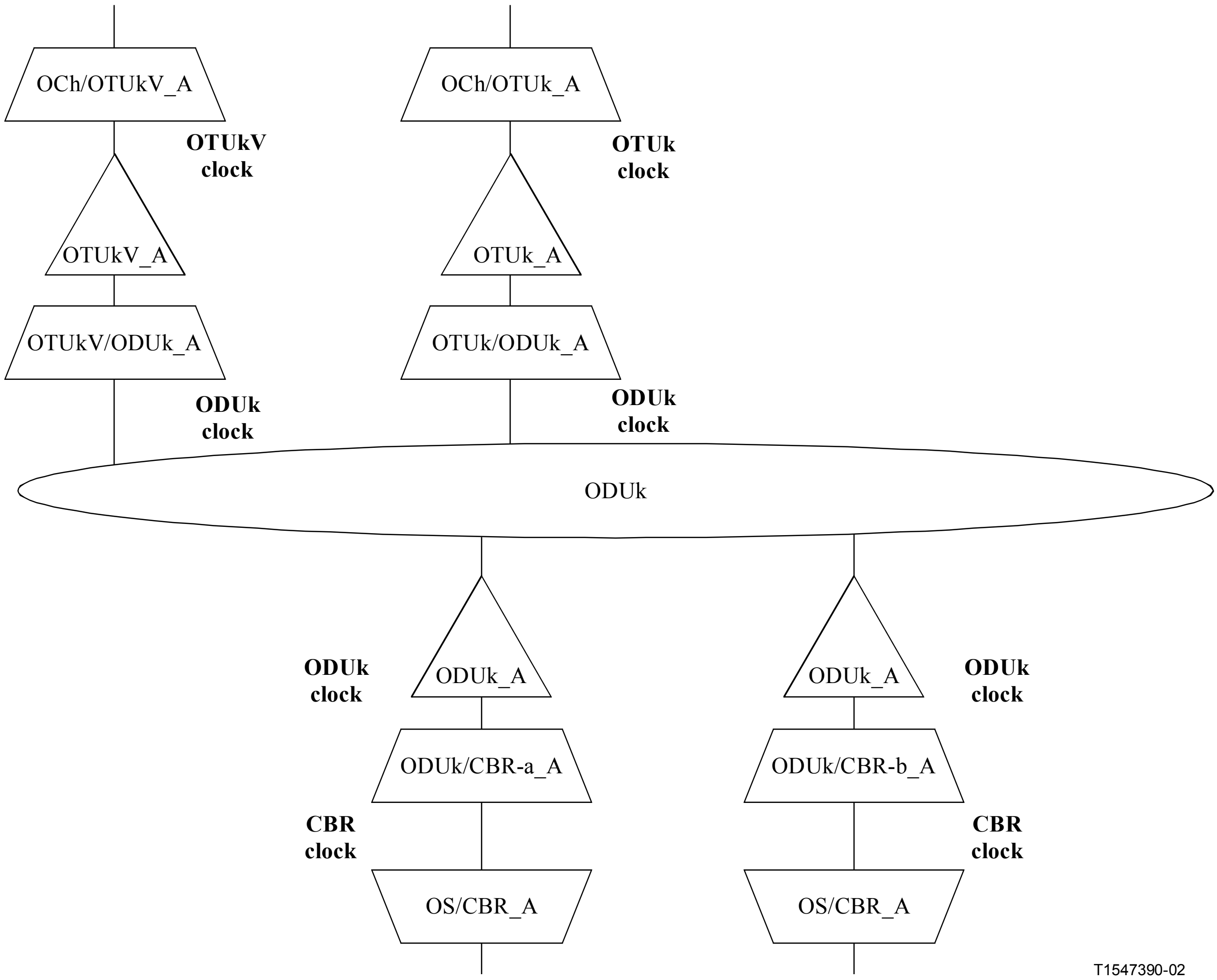

Figure VI.1/G.8251 – Atomic functions used for OTN timing

OCh/OTUk_A_Sk: Clock recovery for the OTUk clock.

OTUk/ODUk_A_Sk: Generates ODUk clock from OTUk clock (255:239 ratio). In case of OTUk defects including signal fail AIS is generate with an AIS clock. The ODUk clock has to be within the limits even in case of a loss of signal.

OTUk/ODUk_A_So: Generates OTUk clock from ODUk clock (239:255 ratio). As the ODUk signal is always available, no AIS clock is required. A switch between several ODUk signals with different clock phases and different frequencies shall not harm the OTUk clock.

OCh/OTUkV_A_Sk: Clock recovery for the OTUkV clock.

OTUkV/ODUk_A_Sk: Generate ODUk clock, either with a fixed ratio (synchronous mapping) or based on the OTUkV clock and stuffing (asynchronous mapping).

OTUkV/ODUk_A_So: Generate ODUkV clock, either from the ODUk clock with a fixed ration (synchronous mapping) or free running (asynchronous mapping) with stuffing of the ODUk into the OTUk.

ODUk/CBR-a_A_So: Generate free running ODUk clock. Stuffing of CBR into ODUk.

ODUk/CBR-b_A_So: Generate ODUk clock from CBR clock (fixed ratio). Generate AIS clock during incoming signal fail (including LOS).

ODUk/CBR_A_Sk: Generate CBR clock based on ODUk clock and stuffing decision. AIS clock on incoming signal fail.

OS/CBR_A_Sk: Clock recovery for CBR signal.

SERIES OF ITU-T RECOMMENDATIONS

Series A	Organization of the work of ITU-T
Series B	Means of expression: definitions, symbols, classification
Series C	General telecommunication statistics
Series D	General tariff principles
Series E	Overall network operation, telephone service, service operation and human factors
Series F	Non-telephone telecommunication services
Series G	**Transmission systems and media, digital systems and networks**
Series H	Audiovisual and multimedia systems
Series I	Integrated services digital network
Series J	Cable networks and transmission of television, sound programme and other multimedia signals
Series K	Protection against interference
Series L	Construction, installation and protection of cables and other elements of outside plant
Series M	TMN and network maintenance: international transmission systems, telephone circuits, telegraphy, facsimile and leased circuits
Series N	Maintenance: international sound programme and television transmission circuits
Series O	Specifications of measuring equipment
Series P	Telephone transmission quality, telephone installations, local line networks
Series Q	Switching and signalling
Series R	Telegraph transmission
Series S	Telegraph services terminal equipment
Series T	Terminals for telematic services
Series U	Telegraph switching
Series V	Data communication over the telephone network
Series X	Data networks and open system communications
Series Y	Global information infrastructure and Internet protocol aspects
Series Z	Languages and general software aspects for telecommunication systems

Printed in Switzerland
Geneva, 2002